LCC-0115
February 2003

Linear Collider Collaboration Tech Notes

Measurement of Vibration Transfer from Surface to Beam Tunnel

Hal Amick, Tao Xu, Nat Wongprasert

Colin Gordon & Associates
883 Sneath Lane, Suite 150
San Bruno CA 94066 USA

Abstract: On 7 August 2002, a vibration measurement program was carried out at SLAC, the purpose of which was to document the vibration attenuation characteristics of the soil at that site. The measurements were carried out by Dr. Tao Xu and Dr. Nat Wongprasert of Colin Gordon & Associates. This report presents data from that study in a somewhat summarized form..

Stanford Linear Accelerator Center (SLAC)
Stanford University

Measurement of Vibration Transfer from Surface to Beam Tunnel

7 August 2002

Prepared by: **Hal Amick**
Tao Xu
Nat Wongprasert

Colin Gordon & Associates
883 Sneath Lane, Suite 150
San Bruno CA 94066 USA
Phone: (650) 358-9577
Facsimile: (650) 358-9430
www.colingordon.com

CG&A Project No. 02074
20 February 2003

Measurement of Vibration Transfer from Surface to Beam Tunnel
Stanford Linear Accelerator Center (SLAC)

7 August 2002

by Hal Amick, Tao Xu and Nat Wongprasert
Colin Gordon & Associates
San Bruno, CA

INTRODUCTION

On 7 August 2002, a vibration measurement program was carried out at SLAC, the purpose of which was to document the vibration attenuation characteristics of the soil at that site. The measurements were carried out by Dr. Tao Xu and Dr. Nat Wongprasert of Colin Gordon & Associates. This report presents data from that study in a somewhat summarized form.

The proposed Next Linear Collider (NLC) will be constructed in a tunnel, but it is yet to be resolved whether this tunnel will be bored at great depth (in rock) or excavated in cut-and-cover construction, at lesser depth. One of the questions to be addressed is whether there is a difference in the vibration attenuation characteristics of the two schemes, with regard to vibrations generated at the surface. Those vibrations may be due to either traffic or mechanical sources.

The purpose of the measurements was to assess the attenuation provided by a cut-and-cover tunnel construction, assuming the SLAC beamline tunnel to be representative of such performance. This report does not address in any way the attenuation that might provided in a bored tunnel in rock.

INSTRUMENTATION

Ground vibration measurements were made with the following equipment:

- Accelerometer - Brüel & Kjær Model 8318 (WH 2146)
- Charge Amplifiers - Brüel & Kjær Model 2635
- Velocity Sensor - Mark Model L-4 Geophone
- Spectrum Analyzer - ACE Data Physics Analyzer
  - Rion SA-77 handheld spectrum analyzer
- Impact Hammers - PCB 2.5 lb hammer with force sensor, and inertia mass model 086C20

- 10lb sledgehammer with a Brüel & Kjær Model 4371 accelerometer attached to one end

- Associated calibration system, cables and connectors.

The velocity sensor was provided by SLAC. The remaining equipment was provided by Colin Gordon & Associates. The calibration of the CG&A measurement instruments, which uses reference standards traceable to NIST, is performed yearly. Simple calibrations were conducted in the field at the time of the measurement survey.

MEASUREMENT PROGRAM

Figure 1 shows the relative locations of sources and receptors. (The scale is in feet.) The receptor locations were on the floor along the centerline of the beam. The sources were on the ground surface. Drive location S1 was at the same approximate elevation as the roadway and the klystron gallery floor, which lies about 36 ft above the elevation of the receptor locations. Drive location S2 was uphill, such that its elevation was about 10 ft higher than S1.

Figure 1. Relative locations (plan view) of sources (S#) and receptors (R#)

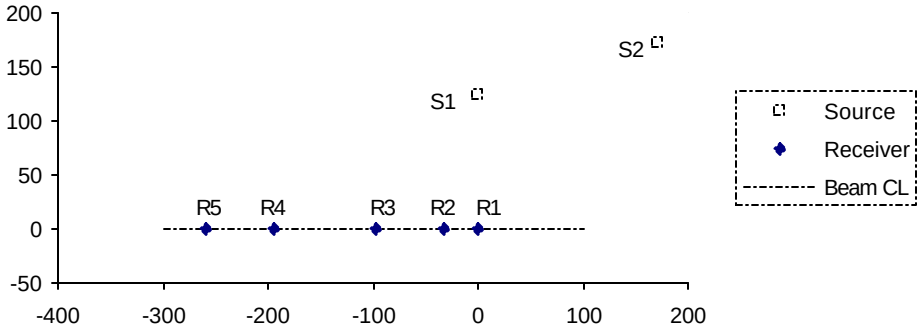

Table 1 summarizes the distances between sources and receivers. The distance includes the change in elevation.

Table 1. Distances between sources and receivers.

Source	Receiver	Distance, ft
S1	R1	130
	R2	134
	R3	162
	R4	233
	R5	289
S2	R1	248
	R2	271

Concrete blocks about 24" x 24" x 12" thick were poured on the ground by SLAC at locations S1 and S2. Steel "anvil" plates were embedded in the top surface of each block. A neoprene pad was placed atop the steel plate, and the hammer struck the pad. The purpose of the pad was to spread the impact out over time, changing the frequency distribution of the impact force. (A softer pad produces more force at low frequencies.)

The tests involved two steps:

(1) Striking the instrumented hammer against the neoprene pad on the concrete block and measuring the vibration response adjacent to the location that was struck. The response curve (velocity divided by the force that was applied by the hammer) is called the "drive point mobility."
(2) Striking the instrumented hammer against the neoprene pad on the block and measuring the vibration response at a receptor location in the tunnel. The response curve in this case (velocity at the receptor location divided by the hammer force) is called the "transfer mobility."

Mobility represents the velocity spectrum produced by a force spectrum with unit amplitude over the full frequency range.

If a transfer mobility spectrum is divided by the corresponding drive point mobility spectrum, the result is a "transfer function" spectrum that relates a velocity spectrum at the receptor to a velocity spectrum of unit amplitude at the drive point. Thus, if we have a velocity spectrum representing vibration response at the drive point to an arbitrary source there, we can multiply that drive point spectrum by the transfer function to obtain the velocity spectrum at the receptor location.

Two-channel spectrum analyzers can be configured to obtain these quantities automatically using the *frequency response function* (FRF). The "response" signal (either the measured source or receptor velocity) is measured simultaneously with the "input" signal (the dynamic force, or in our case, the deceleration of the moving mass of the sledgehammer). The two signals are digitized and a fast Fourier transform (FFT) calculation is used to produce the magnitude and phase of the FRF.

The instrumented hammer produced a voltage output proportional to the force of the blow. This signal originates from a force transducer attached to the hammer when the PCB hammer was used, or when the instrumented sledgehammer was used it is calculated by multiplying the mass of the hammer by the decceleration of the hammer as it strikes the floor.

PRESENTATION OF DATA

Figure 2 shows ambient vibrations measured at locations S1 (top) and R1 (bottom). These are representative of conditions at source and receiver locations, respectively. Both locations are extremely quiet. There was traffic on I-280 at the time the measurements were made, but it lies at a distance of about 1 km from the measurement

locations. At this distance, vibrations from this source would be indistinguishable in the ambient.

Tonal vibrations from rotating mechanical equipment are present, but not of serious amplitude. The two primary tones are at 14.25 Hz (855 rpm) and 28.75 Hz (1725 rpm). The broader peaks between 8 and 9 Hz are associated with a resonance of some sort, not with rotating mechanical equipment.

Figure 3 shows the results of a typical hammerblow. The top trace is a time history – force as a function of time. The bottom trace is a Fast Fourier Transform (FFT) of the force time history.

Figure 4 shows two spectra. One is the ambient measured at receptor location R1. The other is the FFT of the response to several hammerblows. Several observations may be made.

- The ambient was measured with the hand-held Rion SA-77 set at 0-100 Hz, and a short cable. The response was measured with the ACE set at 0-125 Hz, and a very long cable. (The sensor was in the tunnel, the computer with the ACE was near the drive point.) Thus, we have concluded, the "spikes" at 60 Hz and 120 Hz are due to electrical "hum" picked up electromagnetically. It means the data at those frequencies are not good, but other data shouldn't be affected.
- There are peaks centered around 8.75 Hz and at 14.25 Hz in both ambient and response. The amplitudes are nearly identical. There is also a peak at 18.75 Hz in which the amplitude is different, but quite similar. At these frequencies, the response is being governed more by ambient than by the input force, so the transfer functions derived from the response will be invalid. (These frequencies were discussed above.)
- The ambient at frequencies less than 7 Hz (in this case) lies above the response. This suggests that there is some variability to the ambient environment at these low frequencies, and these will degrade the response.

Figure 5 shows a typical drive point mobility measured at drive point S1. This graph shows the velocity amplitude divided by force amplitude (in the frequency domain), which also represents the response to a unit force input.

Figure 6 (top) shows a typical transfer mobility measured at R1 due to hammerblows at S1. It is due to multiple blows. The spikes at 60 Hz and 120 Hz are due to electrical noise, as discussed above. The bottom graph shows the quantity called *coherence*, a measure of the "quality" of the transfer mobility. Strictly speaking, it shows, frequency by frequency, how the response signal correlates to the input signal. It varies from 0 to 1, representing a continuum from uncorrelated to fully correlated. Coherence above 0.9 is generally quite good under any circumstances, and those above 0.8 or so are generally good under outdoor field conditions. Dips may be seen at 60 and 120 Hz and the other frequencies at which mechanical systems are generating higher levels than the hammerblows (see above). Also, one may observe rather poor coherence at frequencies below 10 Hz; this is not uncommon in field situations. It takes very heavy blows with a large mass to excite these frequencies in the ground.

The most significant data in the following discussion are in terms of *change* in amplitude between drive and receiver locations. This is obtained by dividing the transfer mobility by the drive point mobility. The change in amplitude is thus unitless, and is sometimes discussed in terms of decibels. Figure 7 (top) shows this quantity. The bottom plot shows the coherence associated with the two mobility curves used for the calculation.

Raw Data

Figures 8 through 22 give the transfer functions (showing change of amplitude) measured at R1 through R5 using S1 as drive point. They are in groups of three, each showing the data in a slightly different manner:

1. The top graph shows three transfer functions calculated from three separate tests, conducted consecutively. The bottom graph shows the corresponding coherence spectra for the drive point and receiver location. The frequency axis is linear.
2. The graph shows the same data as the top graph on the preceding page, except that the frequency axis is logarithmic.
3. The graph shows the log mean (mean of the logs of the three amplitudes) spectrum. The spikes at 60 Hz and 120 Hz (line frequency and harmonic) are excised.

Figures 23 through 28 show the data for which S2 was the drive point, in the format described above. Only two receiver locations were documented. The remainder had coherence significantly below 0.7.

The following table cross-references the figure numbers to the locations and the graph format.

Measurement	From S1 to …					S2 to …	
	R1	R2	R3	R4	R5	R1	R2
Three raw transfer functions, coherence, linear frequency axis	8	11	14	17	20	23	26
Three raw transfer functions, coherence, linear frequency axis	9	12	15	18	21	24	27
Log mean transfer function, log axis	10	13	16	19	22	25	28

Figure 29 presents together the log mean transfer functions for which S1 was the drive point. One can see trends at some frequencies, but the spectra are so "ragged" that the trends are difficult to observe with any clarity.

Smoothed Data

In order to more clearly observe trends, data smoothing of a sort was employed. Figure 30 shows smoothed spectra which were calculated by log averaging the amplitudes over a 3.5 Hz interval centered on the plotted point. There is still some scatter, but the process

added some clarity. Figures 31 and 32 show the same data but with increasing degrees of smoothing (6.5 Hz and 10 Hz intervals).

Figures 33 through 36 show a similar sequence for data measured between S2 and two receptor locations.

DISCUSSION

There are fundamental differences between the transfer functions using S1 as a source and those using S2. They are quite dissimilar. We believe this to be attributable to the difference in paths, because of the proximity of the experimental side tunnel at the second setup locations. Thus, we believe the data with drive point S1 to be more indicative of the case in general.

The following table summarizes the apparent attenuation at several frequencies at which mechanical equipment usually operates. Data are taken from the "Heavily Smoothed" graphs.

Source	Receiver	Distance, ft	Attenuation at Given Frequency			
			10 Hz	20 Hz	30 Hz	60 Hz
S1	R1	130	0.024	0.0084	0.012	0.005
	R2	134	0.012	0.012	0.014	0.004
	R3	162	0.011	0.0084	0.006	0.001
	R4	233	0.010	0.004	0.002	0.001
	R5	289	0.005	0.002	0.009	0.0003
S2	R1	248	0.023	0.011	0.007	0.006
	R2	271	0.027	0.011	0.007	0.006

The figures in the preceding table represent the attenuation factor *A* for a vibration with its source near Sn propagating along the same path. Suppose a pump is installed at S1, and it produces a vibration at 30 Hz of amplitude X. The amplitude at 30 Hz that we would measure at R5 would be the greater of either ambient or 0.009X. Suppose we take the ambient measurement shown for the tunnel (in Figure 2) as representative the tunnel in general. The amplitude at 30 Hz, in the absence of the tones there now, would be about 0.6 μin/s. If we wanted to place a pump at S1 and be sure to avoid having its vibration exceed ambient at R5, we would need to impose a limit on the resulting vibration at S1 of 0.6 / 0.009 = 67 μin/s.

Figure 2: Ground Transmission - SLAC Cut-and-Cover Tunnel - 7 Aug 2002
Ambient Vibrations at Drive Point and Receiver Location R1

a) Drive Point S1

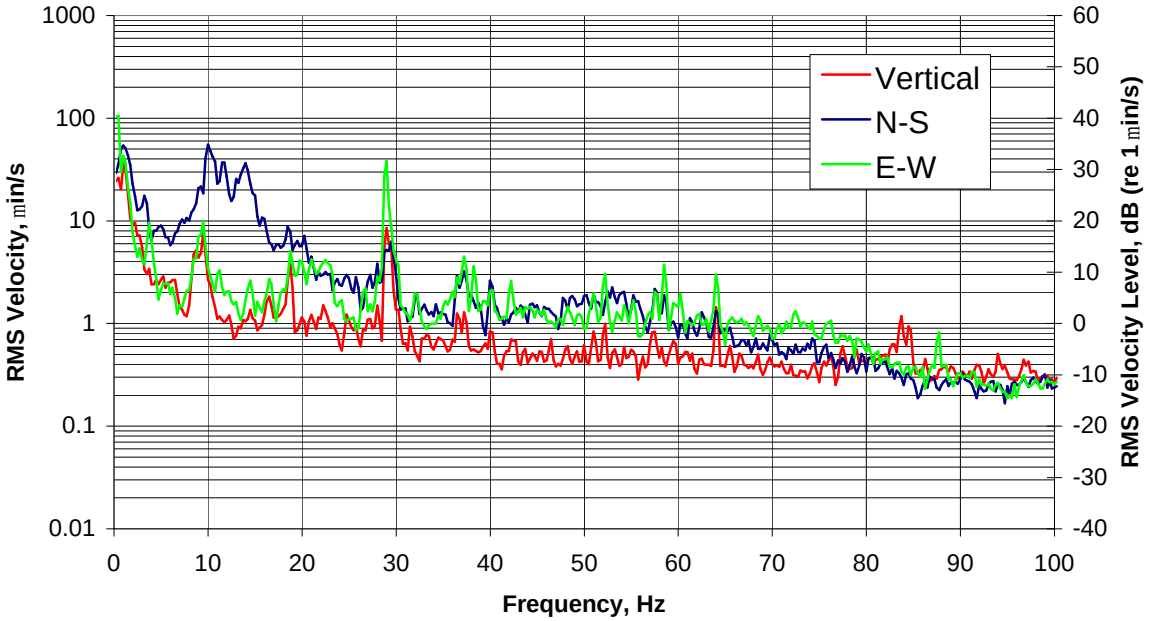

b) Tunnel Receiver Location R1

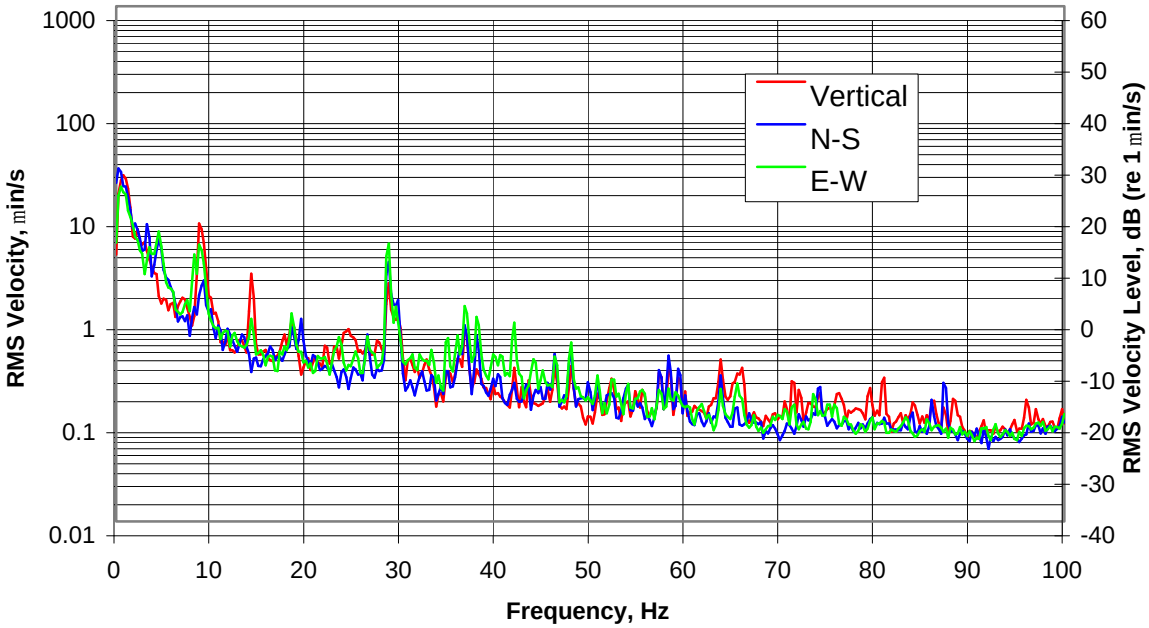

Figure 3: Ground Transmission - SLAC Cut-and-Cover Tunnel - 7 Aug 2002
Typical Hammer Force Time History and Spectrum

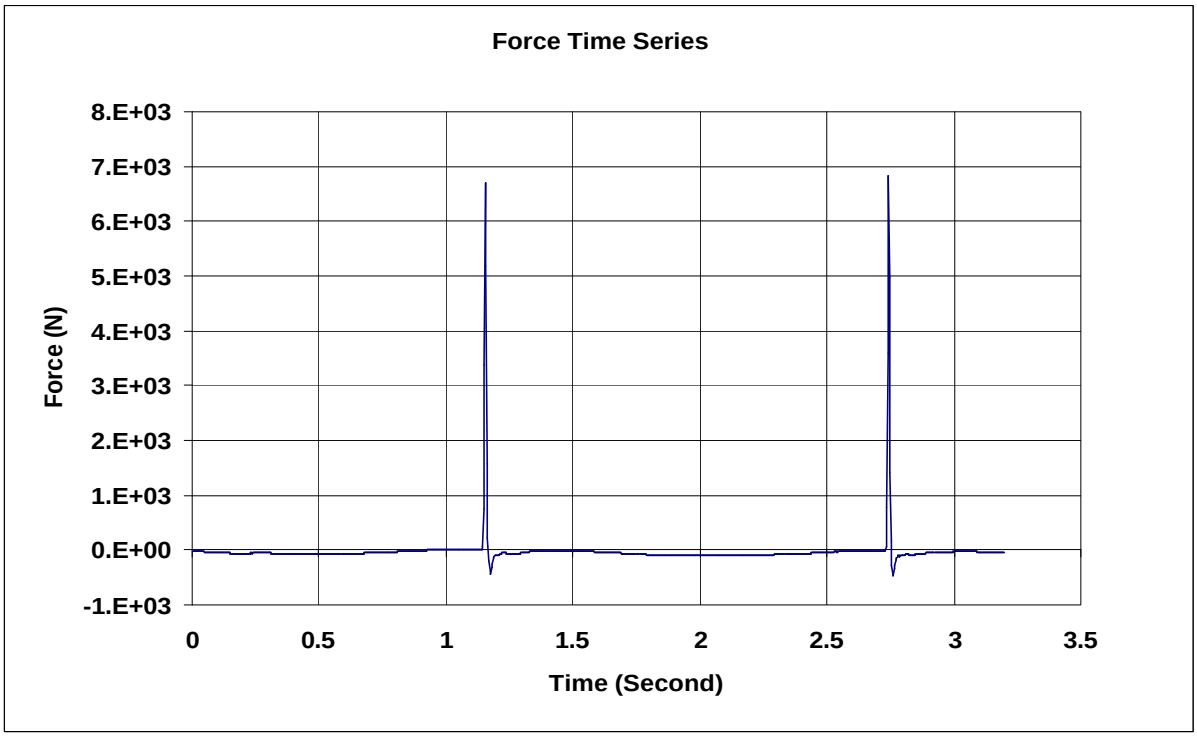

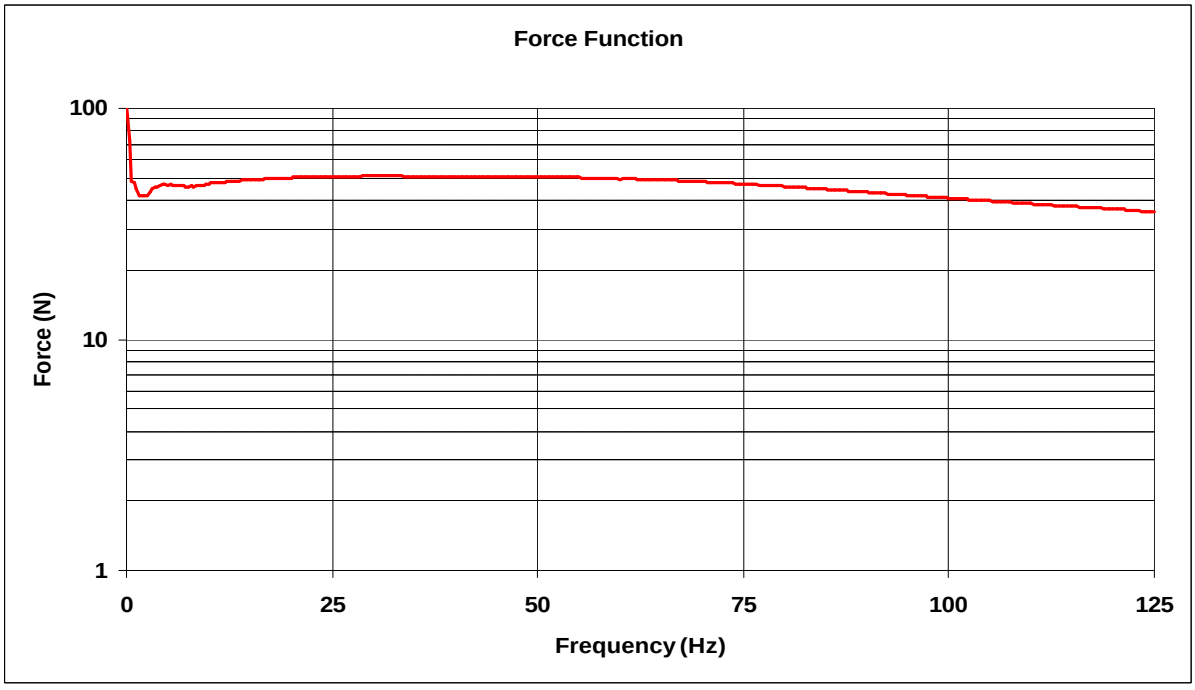

Figure 4: Ground Transmission - SLAC Cut-and-Cover Tunnel - 7 Aug 2002
Typical Reponse at R1 to Hammerblow at S1, with Ambient at R1

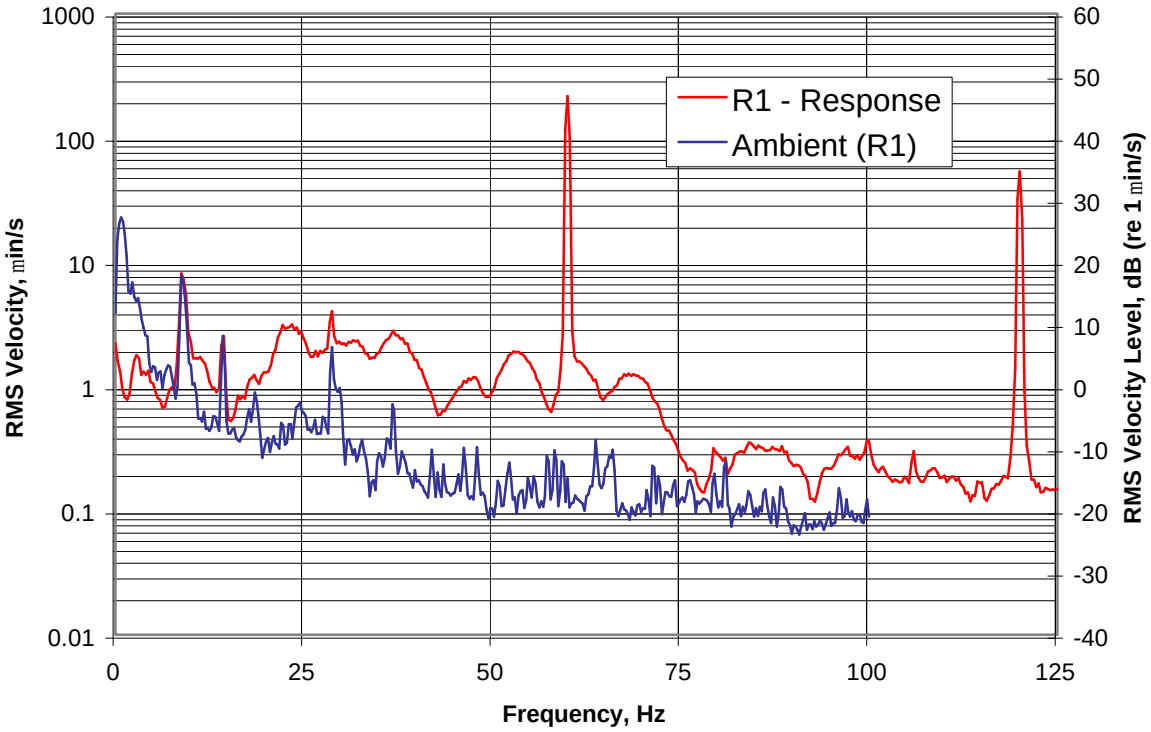

Figure 5: Ground Transmission - SLAC Cut-and-Cover Tunnel - 7 Aug 2002
Drive-Point Mobility at S1

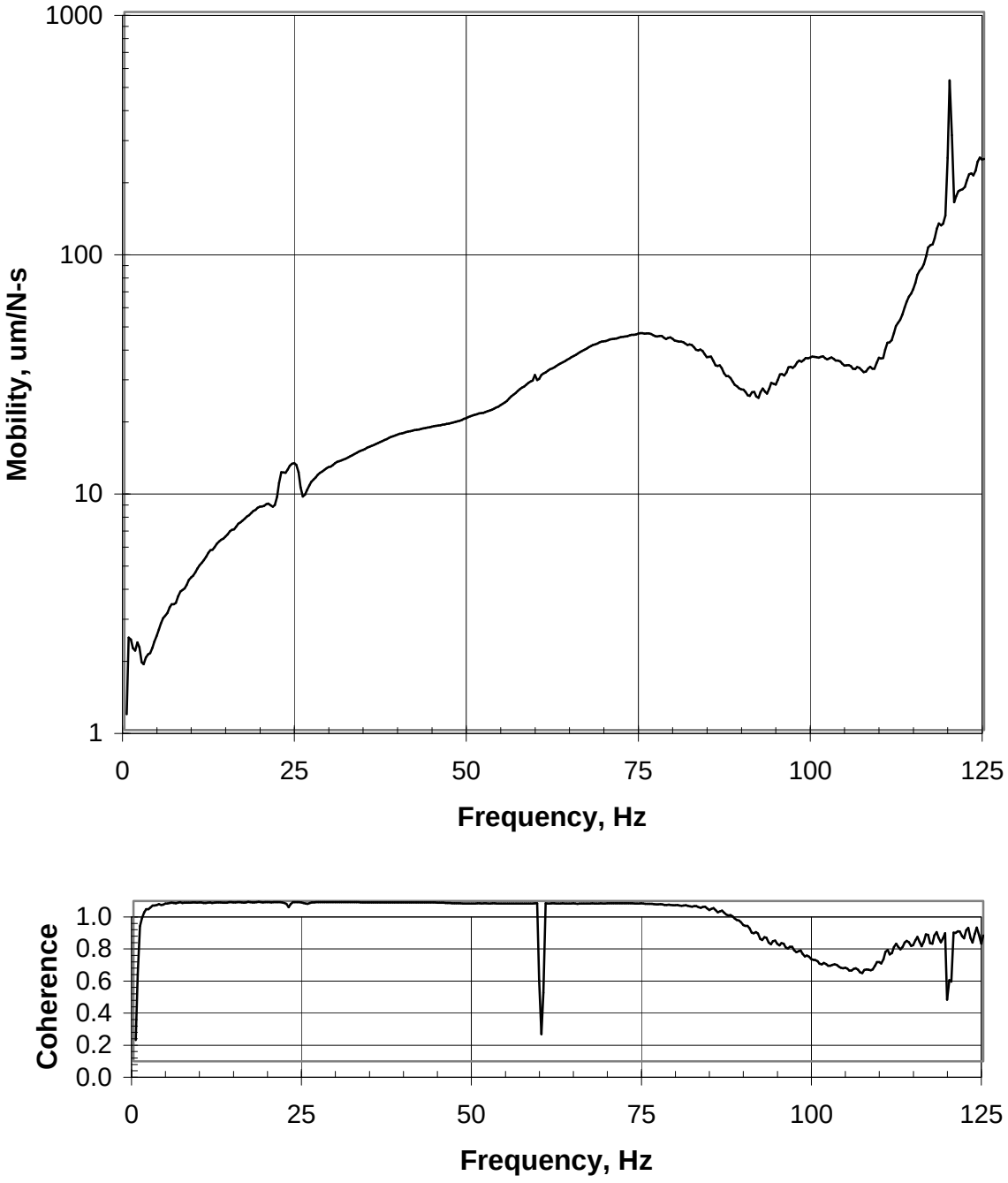

Figure 6: Ground Transmission - SLAC Cut-and-Cover Tunnel - 7 Aug 2002
Transfer Mobility - Response at R1 due to Hammer Force at S1

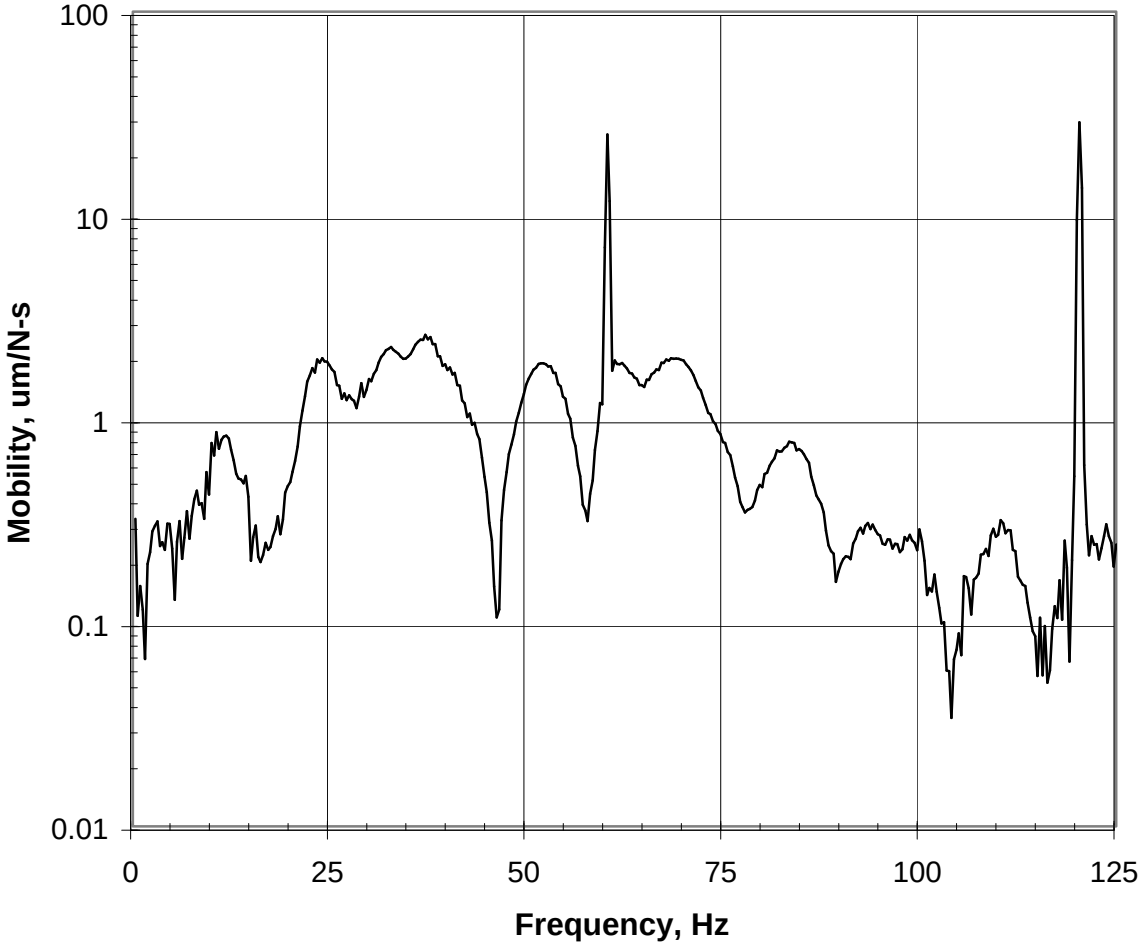

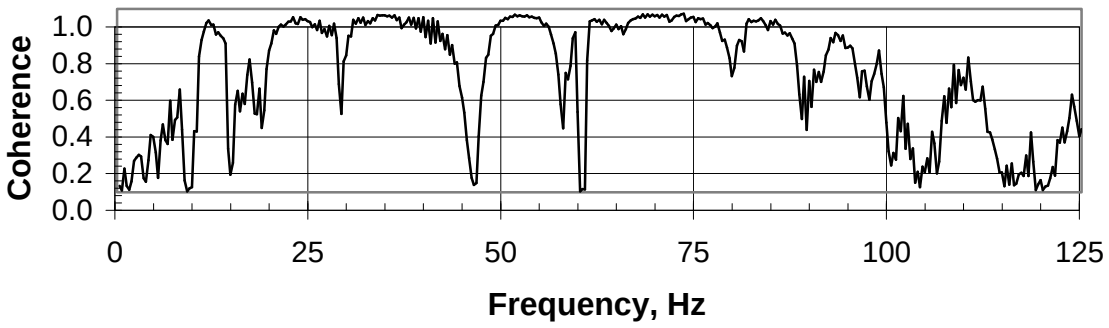

Figure 7: Ground Transmission - SLAC Cut-and-Cover Tunnel - 7 Aug 2002
Transfer Function - Change in Amplitude S1 to R1 due to Hammer Force at S1

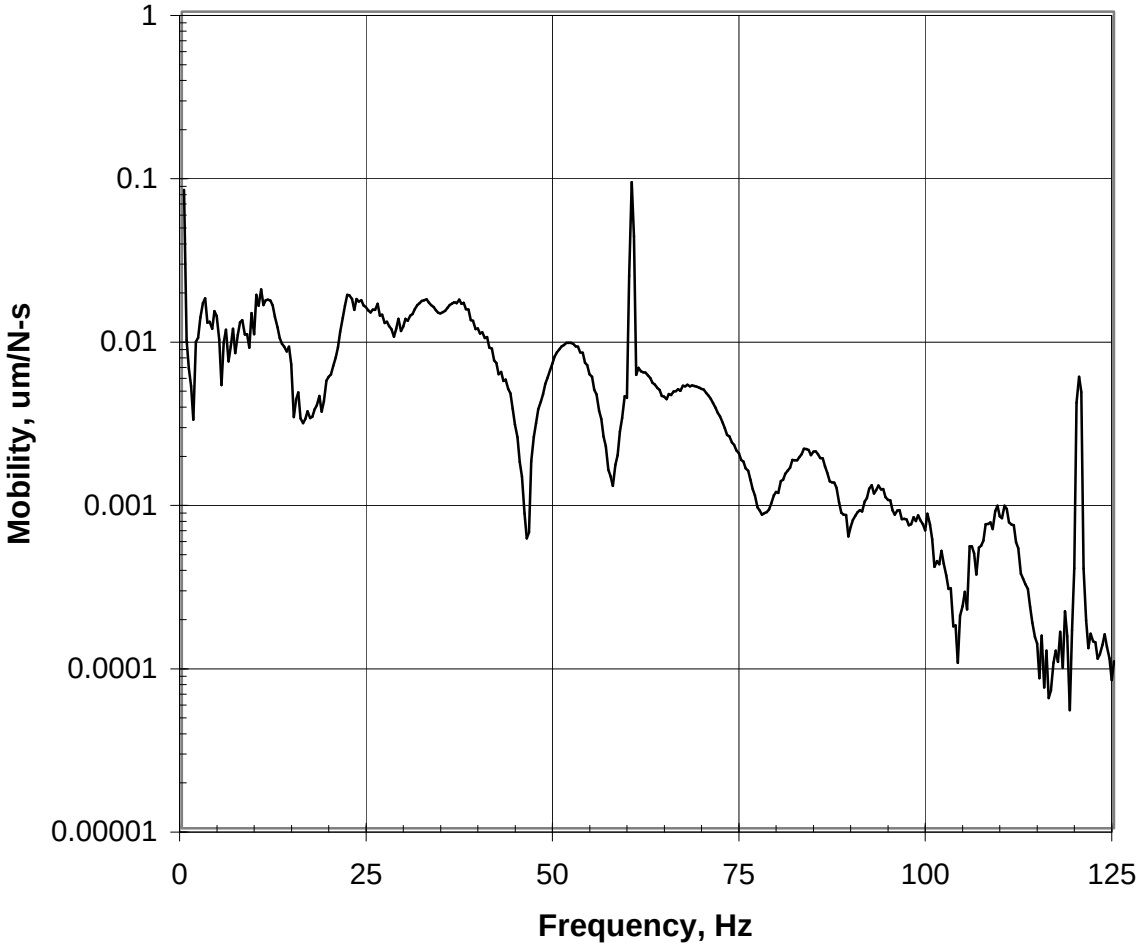

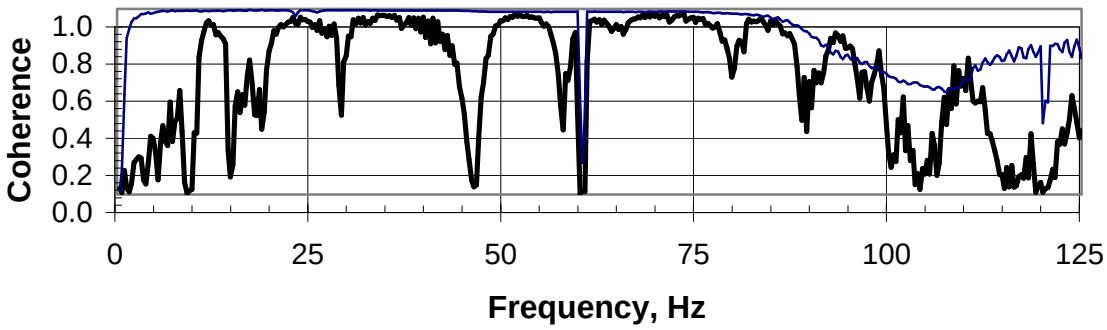

Figure 8: Ground Transmission - SLAC Cut-and-Cover Tunnel - 7 Aug 2002
Transmission from Drive Point S1 to Closest Point in Tunnel R1

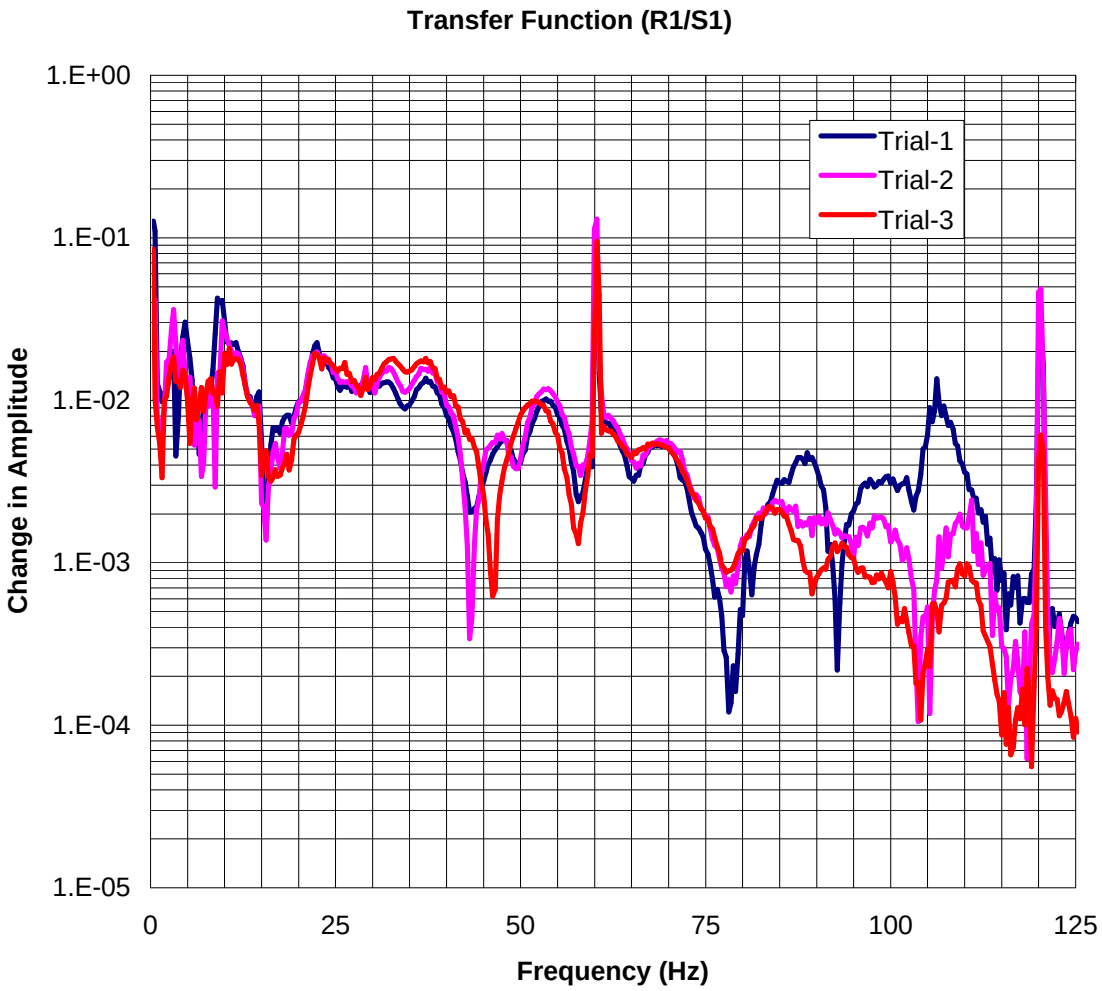

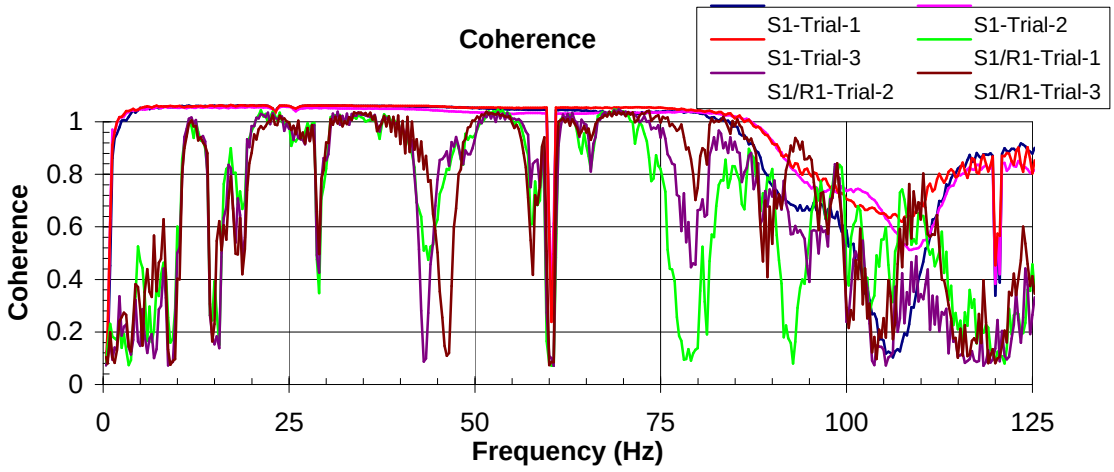

Figure 9: Ground Transmission - SLAC Cut-and-Cover Tunnel - 7 Aug 2002
Transmission from Drive Point S1 to Closest Point in Tunnel R1

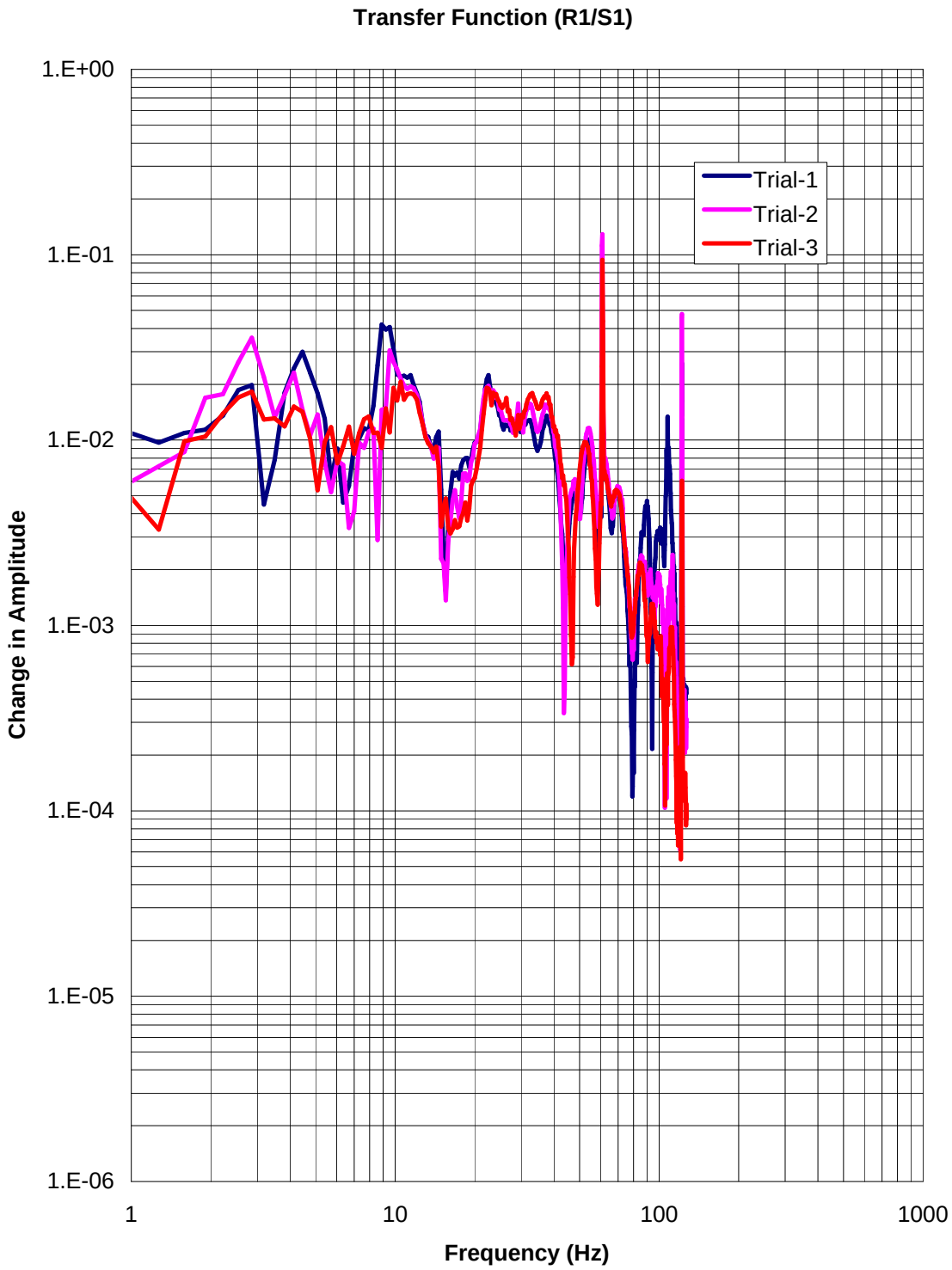

Figure 10: Ground Transmission - SLAC Cut-and-Cover Tunnel - 7 Aug 2002
Transmission from Drive Point S1 to Closest Point in Tunnel R1

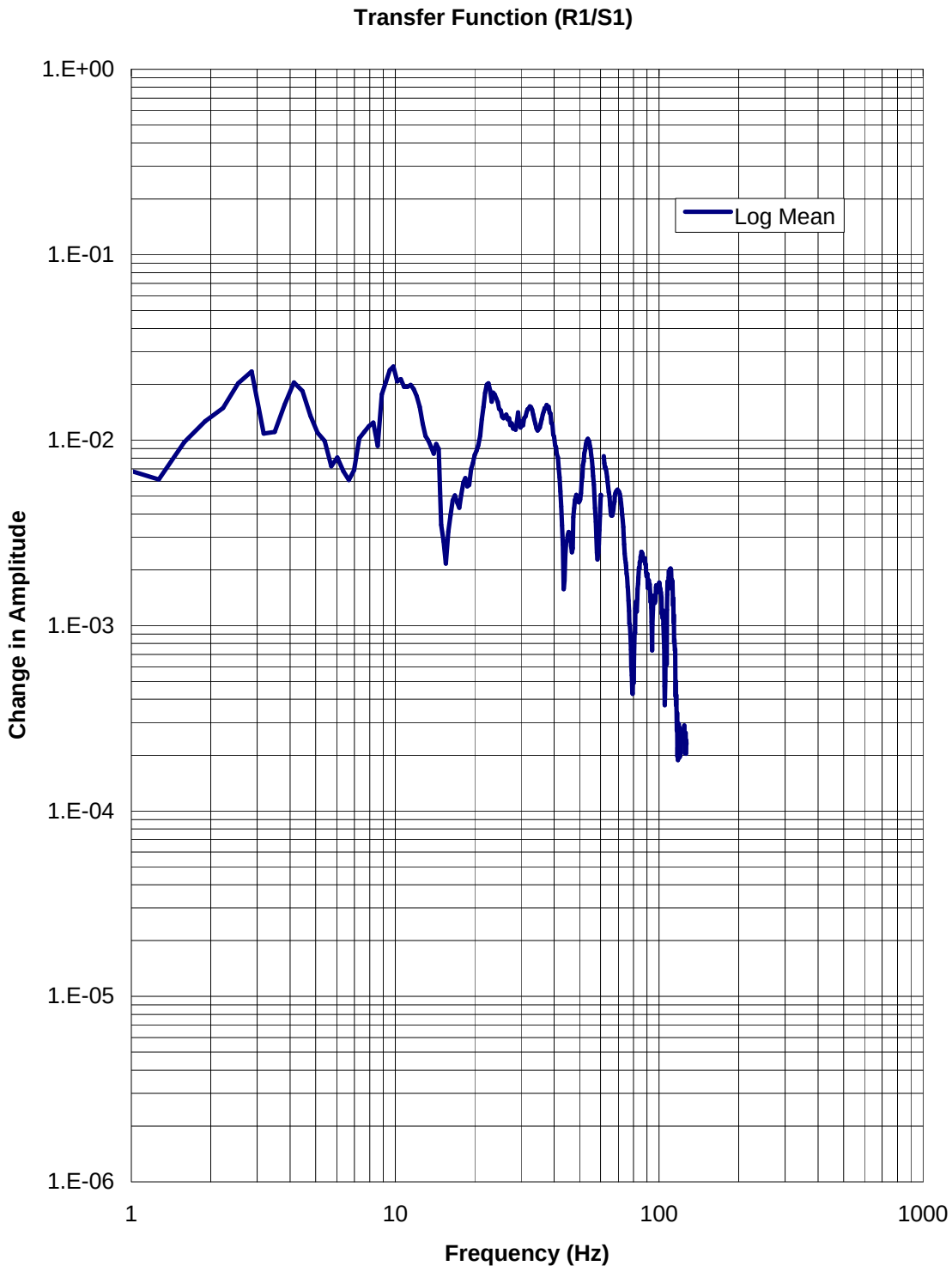

Figure 11: Ground Transmission - SLAC Cut-and-Cover Tunnel - 7 Aug 2002
Transmission from Drive Point S1 to Point in Tunnel R2 (10 m away from R1)

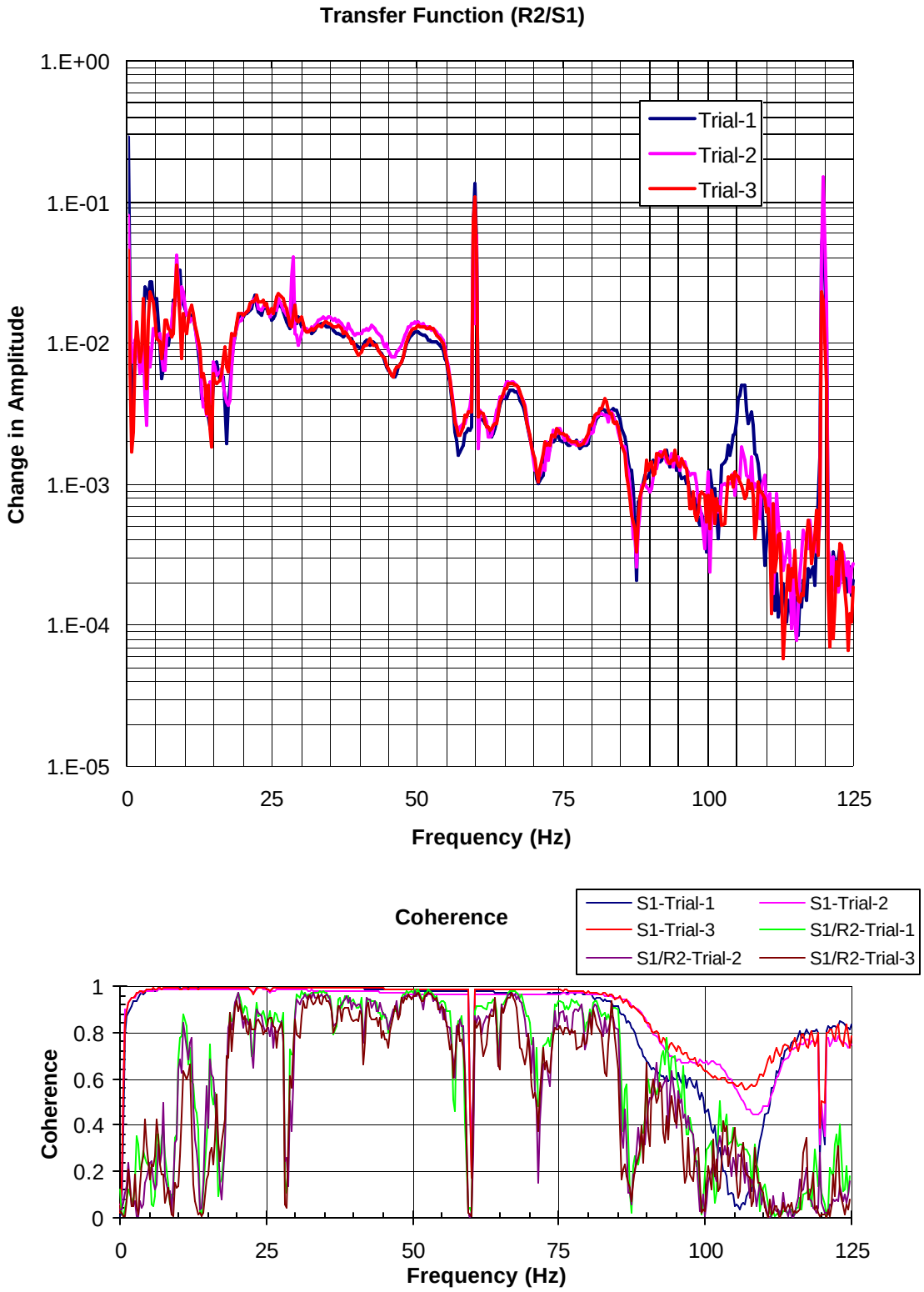

Figure 12: Ground Transmission - SLAC Cut-and-Cover Tunnel - 7 Aug 2002
Transmission from Drive Point S1 to Point in Tunnel R2 (10m away from R1)

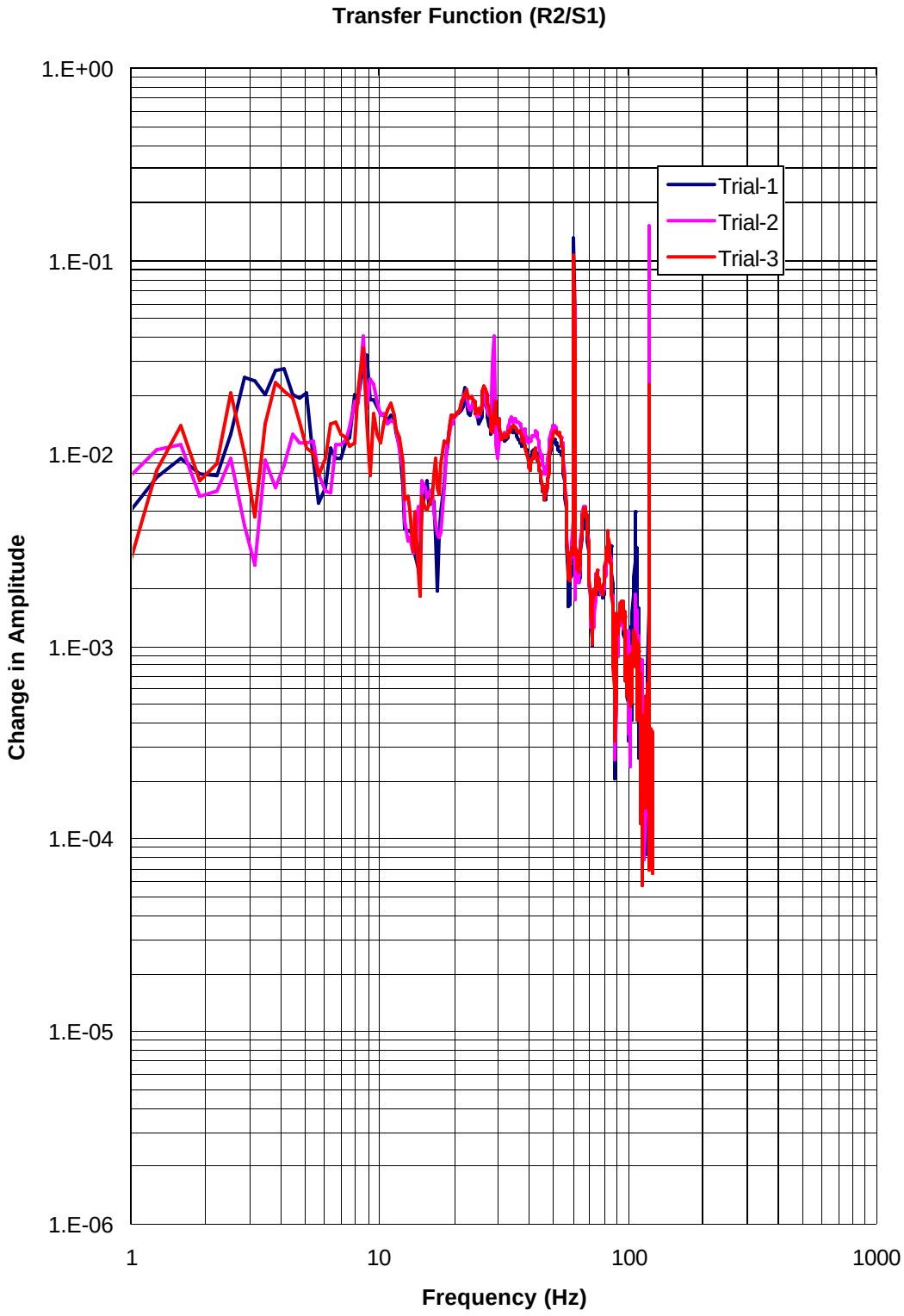

Figure 13: Ground Transmission - SLAC Cut-and-Cover Tunnel - 7 Aug 2002
Transmission from Drive Point S1 to Point in Tunnel R2 (10m away from R1)

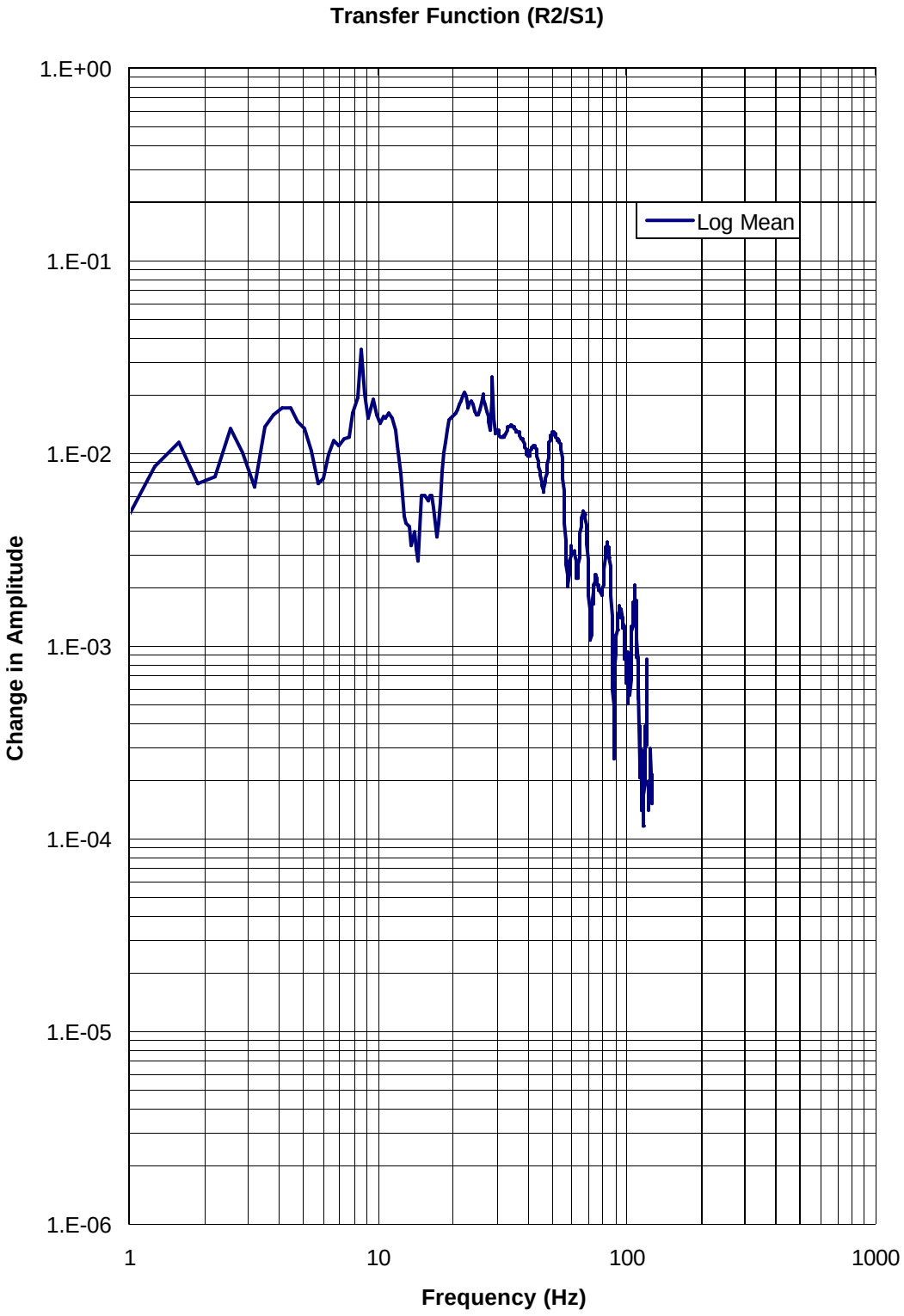

Figure 14: Ground Transmission - SLAC Cut-and-Cover Tunnel - 7 Aug 2002
Transmission from Drive Point S1 to Point in Tunnel R3 (30 m away from R1)

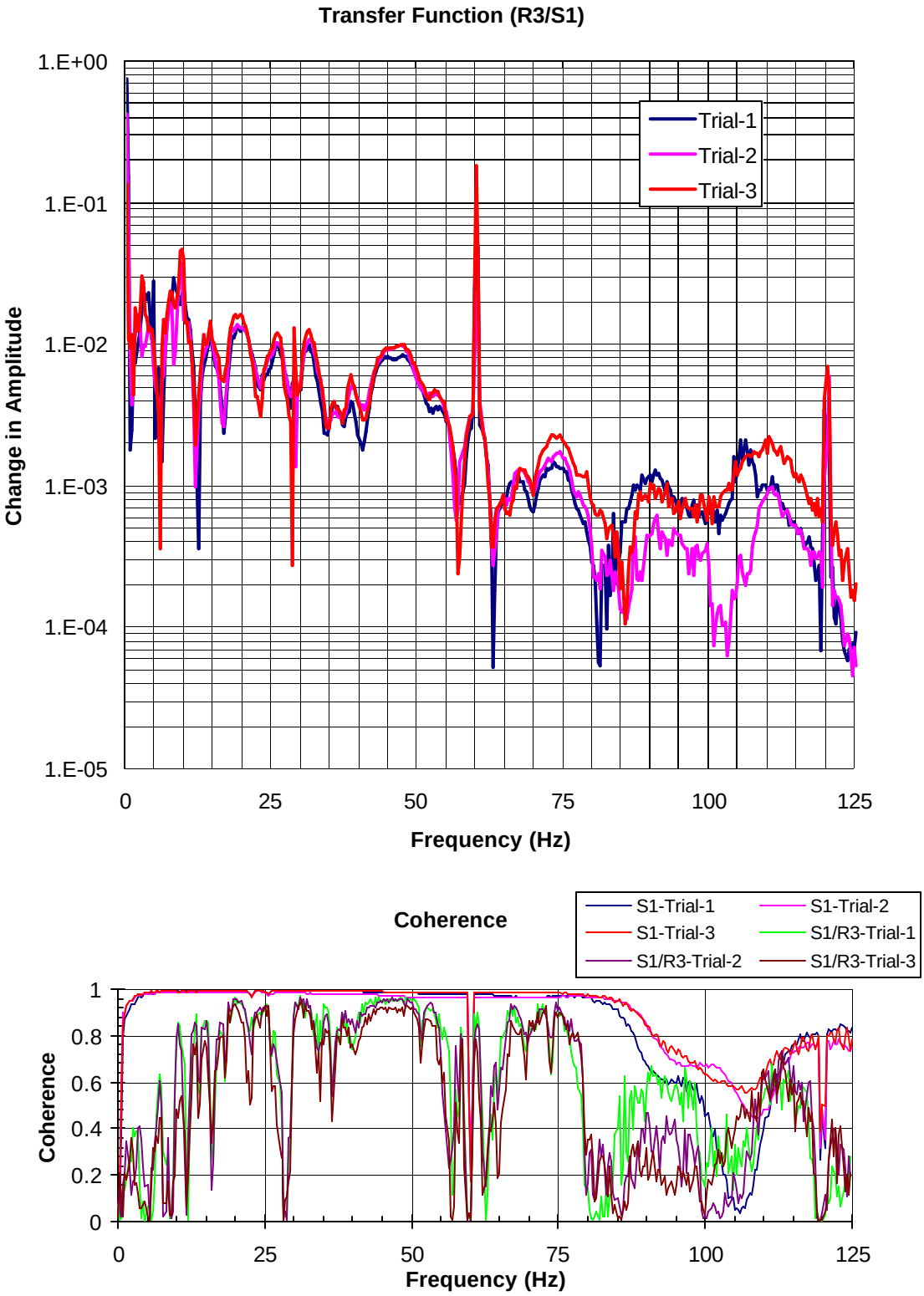

Figure 15: Ground Transmission - SLAC Cut-and-Cover Tunnel - 7 Aug 2002
Transmission from Drive Point S1 to Point in Tunnel R3 (30m away from R1)

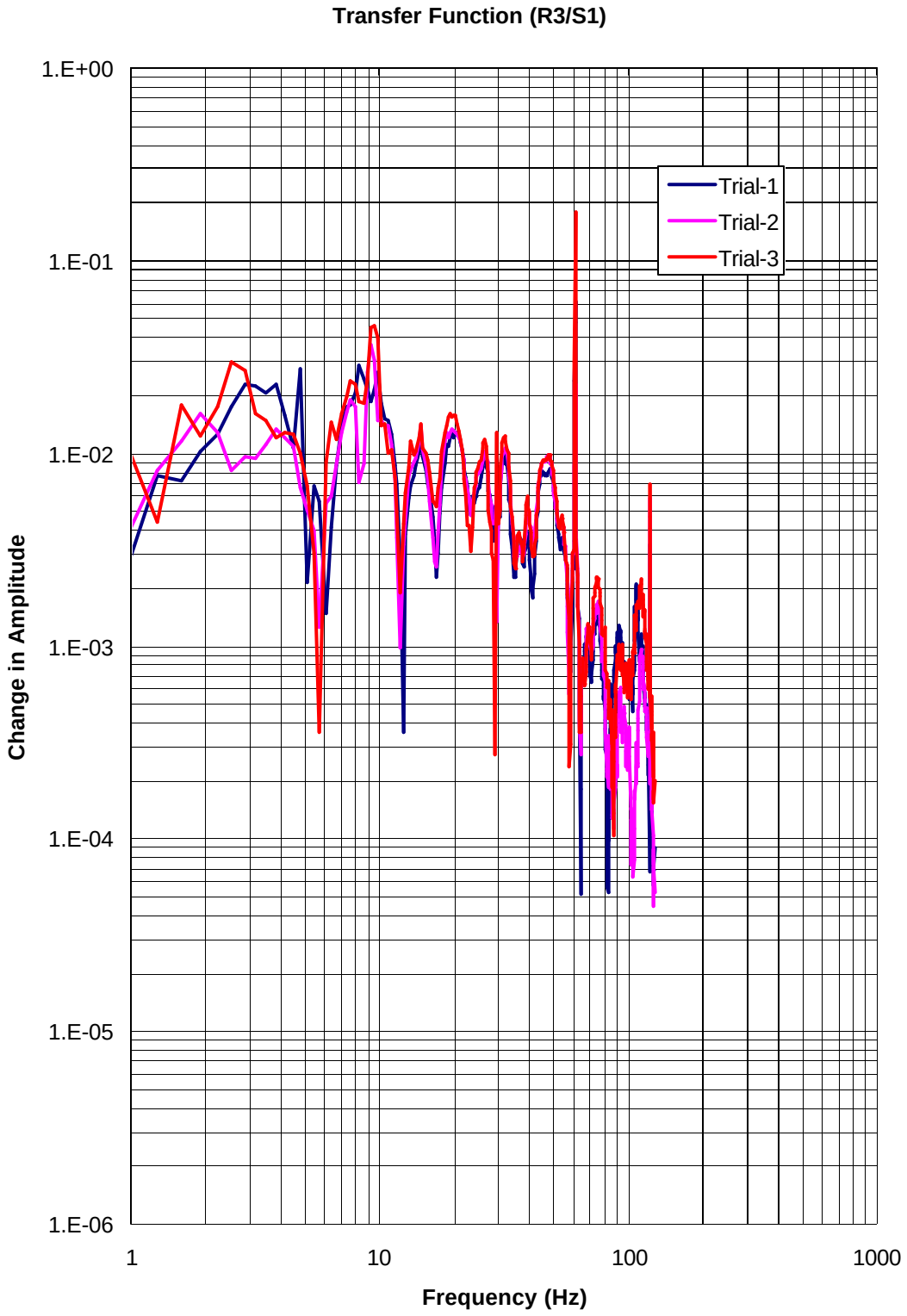

Figure 16: Ground Transmission - SLAC Cut-and-Cover Tunnel - 7 Aug 2002
Transmission from Drive Point S1 to Point in Tunnel R3 (30m away from R1)

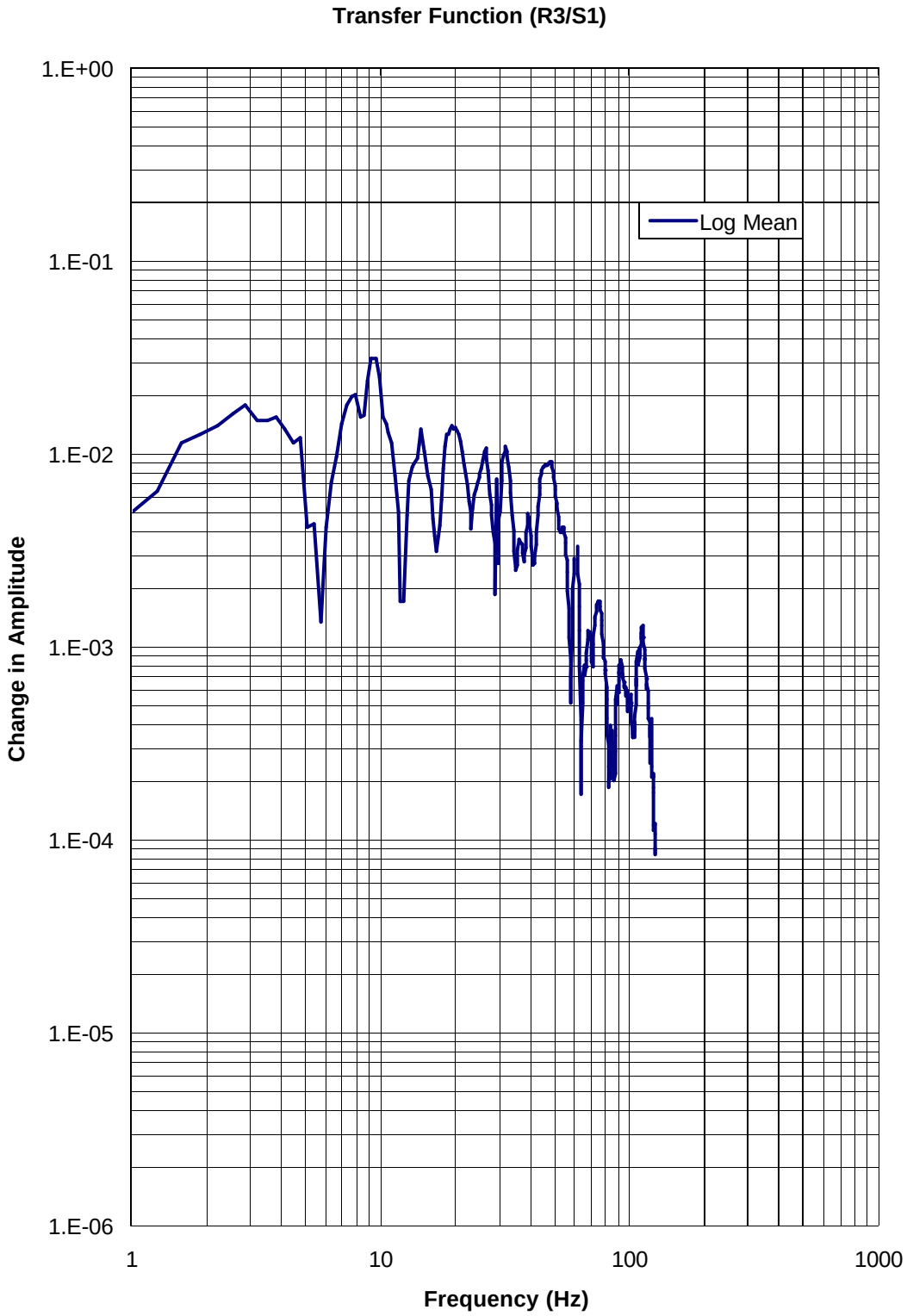

Figure 17: Ground Transmission - SLAC Cut-and-Cover Tunnel - 7 Aug 2002
Transmission from Drive Point S1 to Point in Tunnel R4 (60 m away from R1)

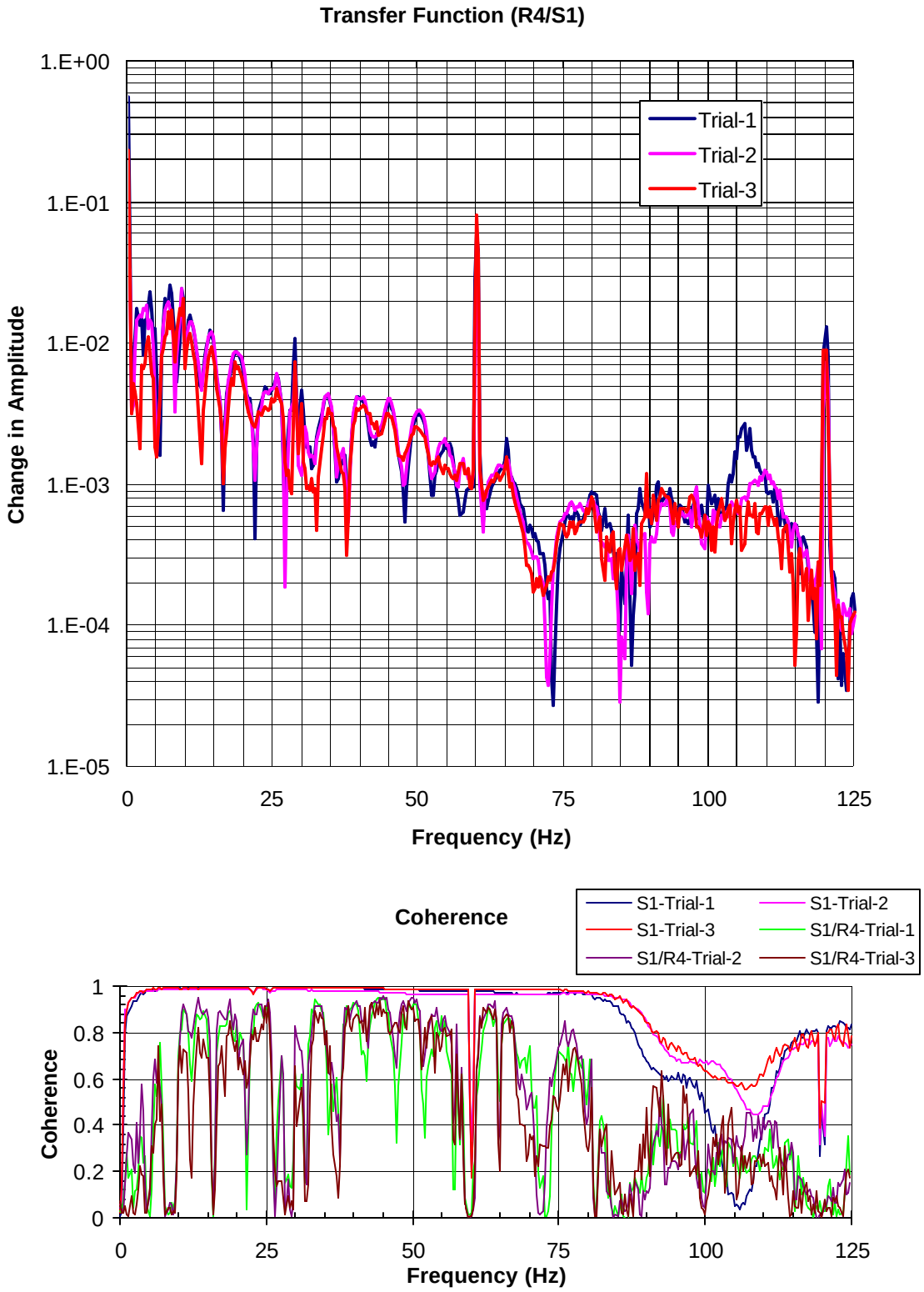

Figure 18: Ground Transmission - SLAC Cut-and-Cover Tunnel - 7 Aug 2002
Transmission from Drive Point S1 to Point in Tunnel R4 (60m away from R1)

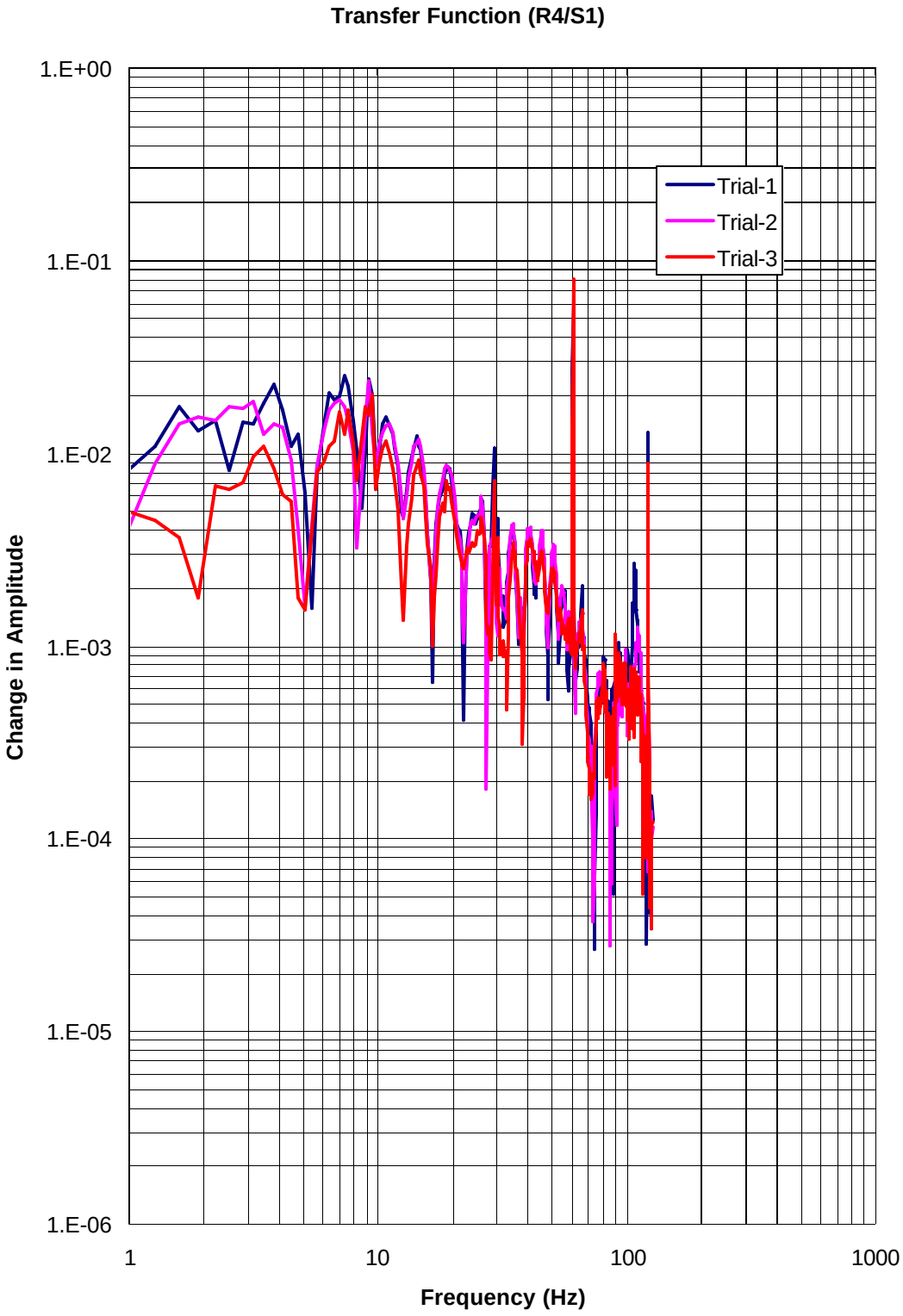

Figure 19: Ground Transmission - SLAC Cut-and-Cover Tunnel - 7 Aug 2002
Transmission from Drive Point S1 to Point in Tunnel R4 (60m away from R1)

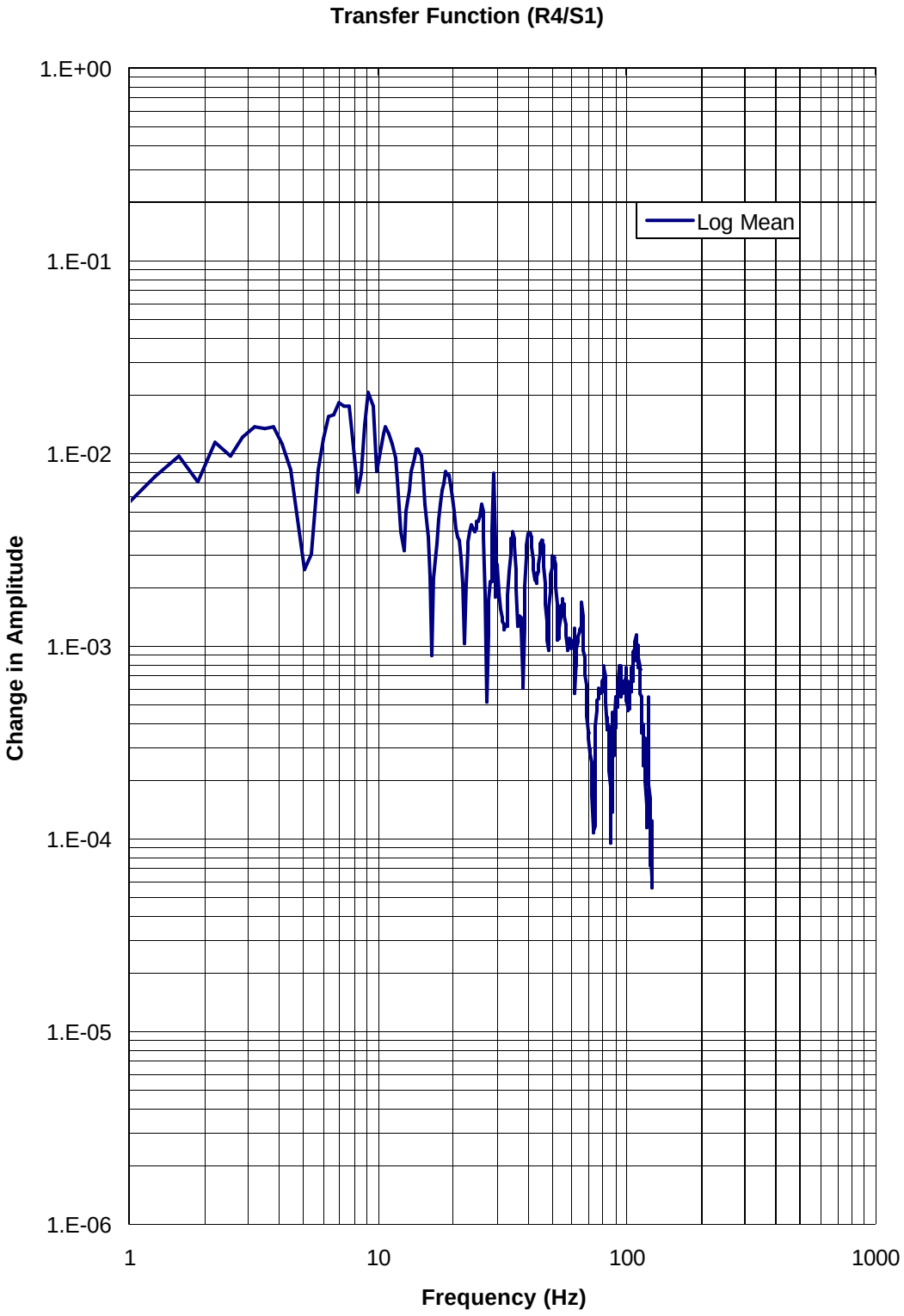

Figure 20: Ground Transmission - SLAC Cut-and-Cover Tunnel - 7 Aug 2002
Transmission from Drive Point S1 to Point in Tunnel R5 (80 m away from R1)

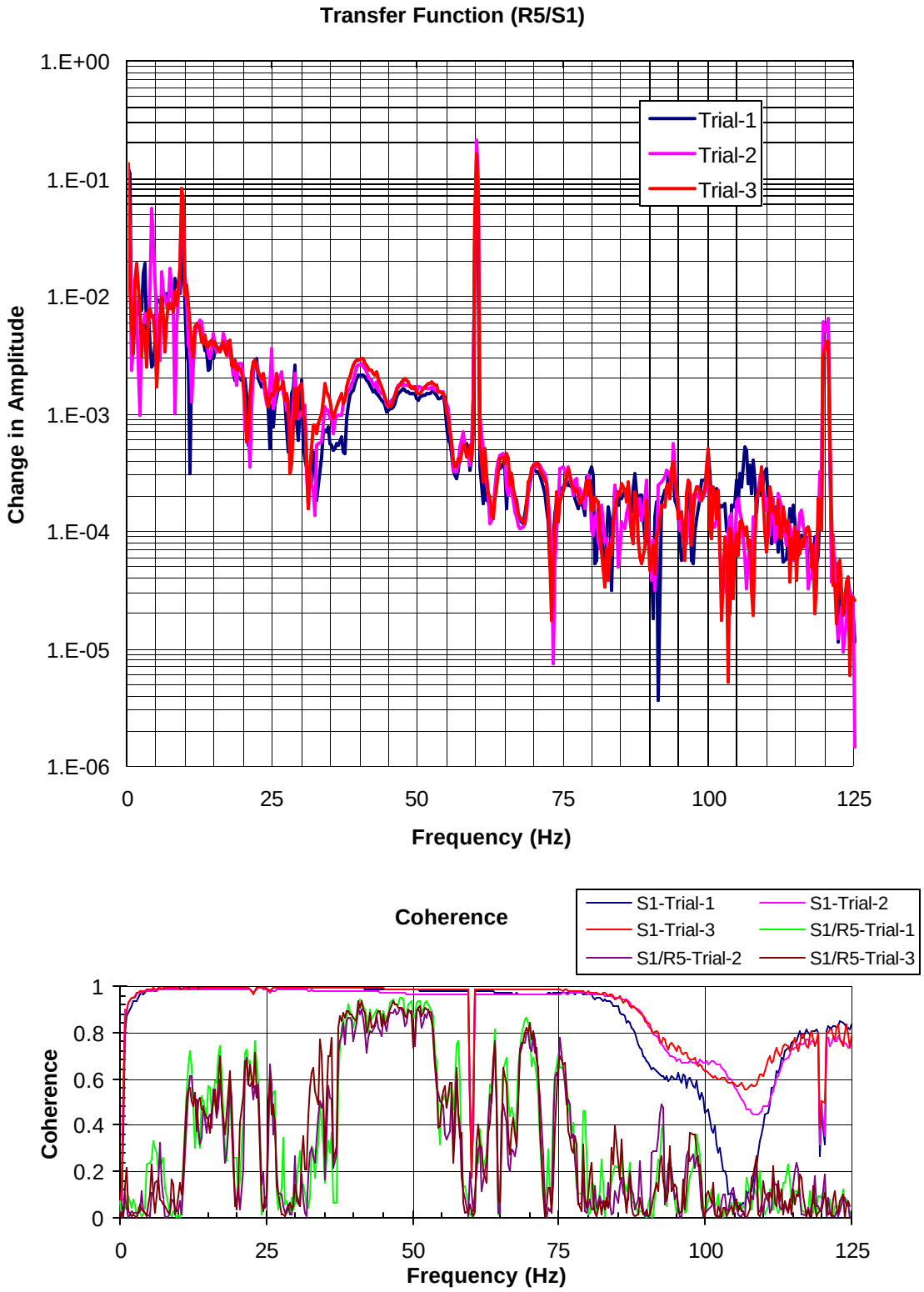

Figure 21: Ground Transmission - SLAC Cut-and-Cover Tunnel - 7 Aug 2002
Transmission from Drive Point S1 to Point in Tunnel R5 (80m away from R1)

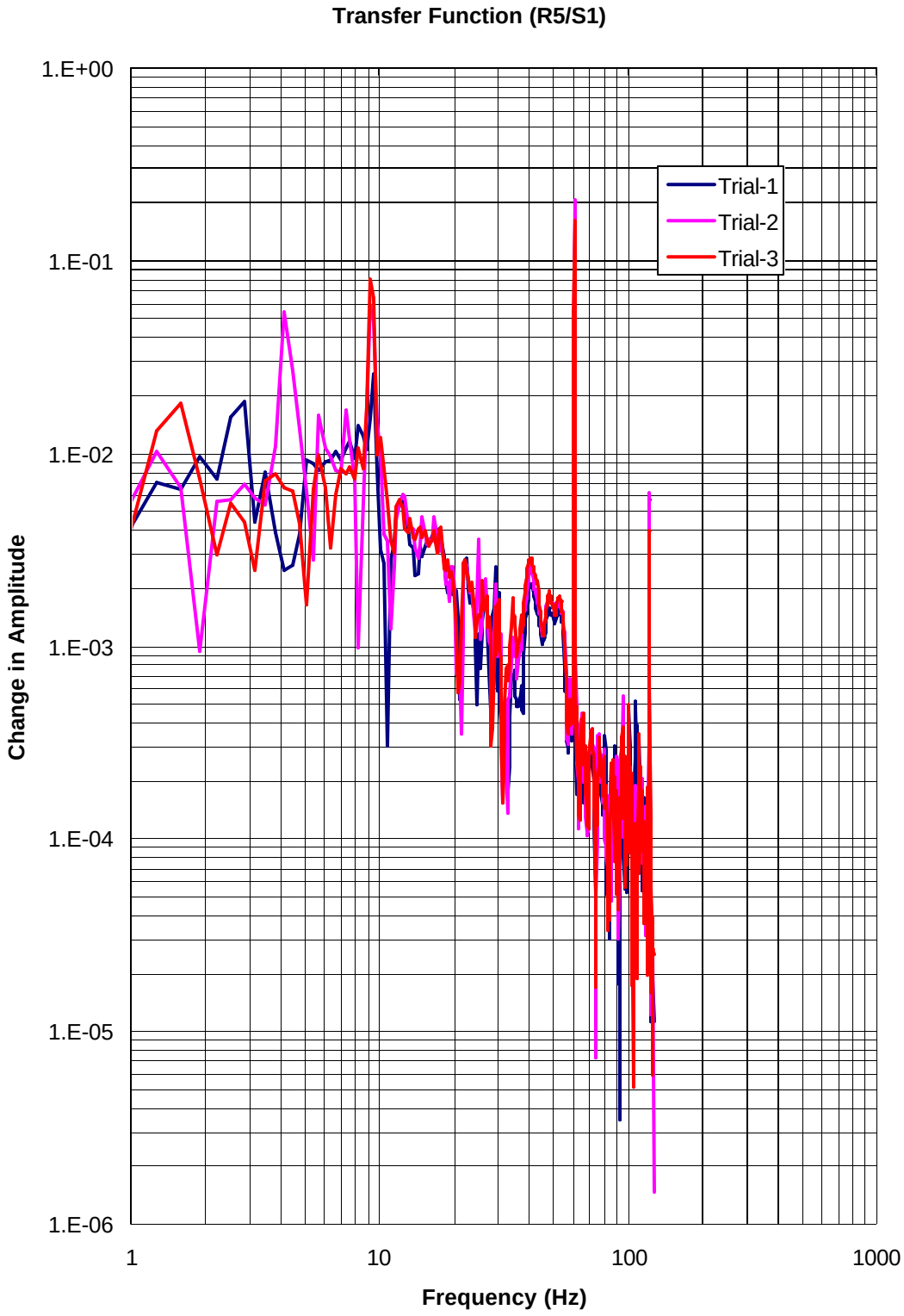

Figure 22: Ground Transmission - SLAC Cut-and-Cover Tunnel - 7 Aug 2002
Transmission from Drive Point S1 to Point in Tunnel R5 (80m away from R1)

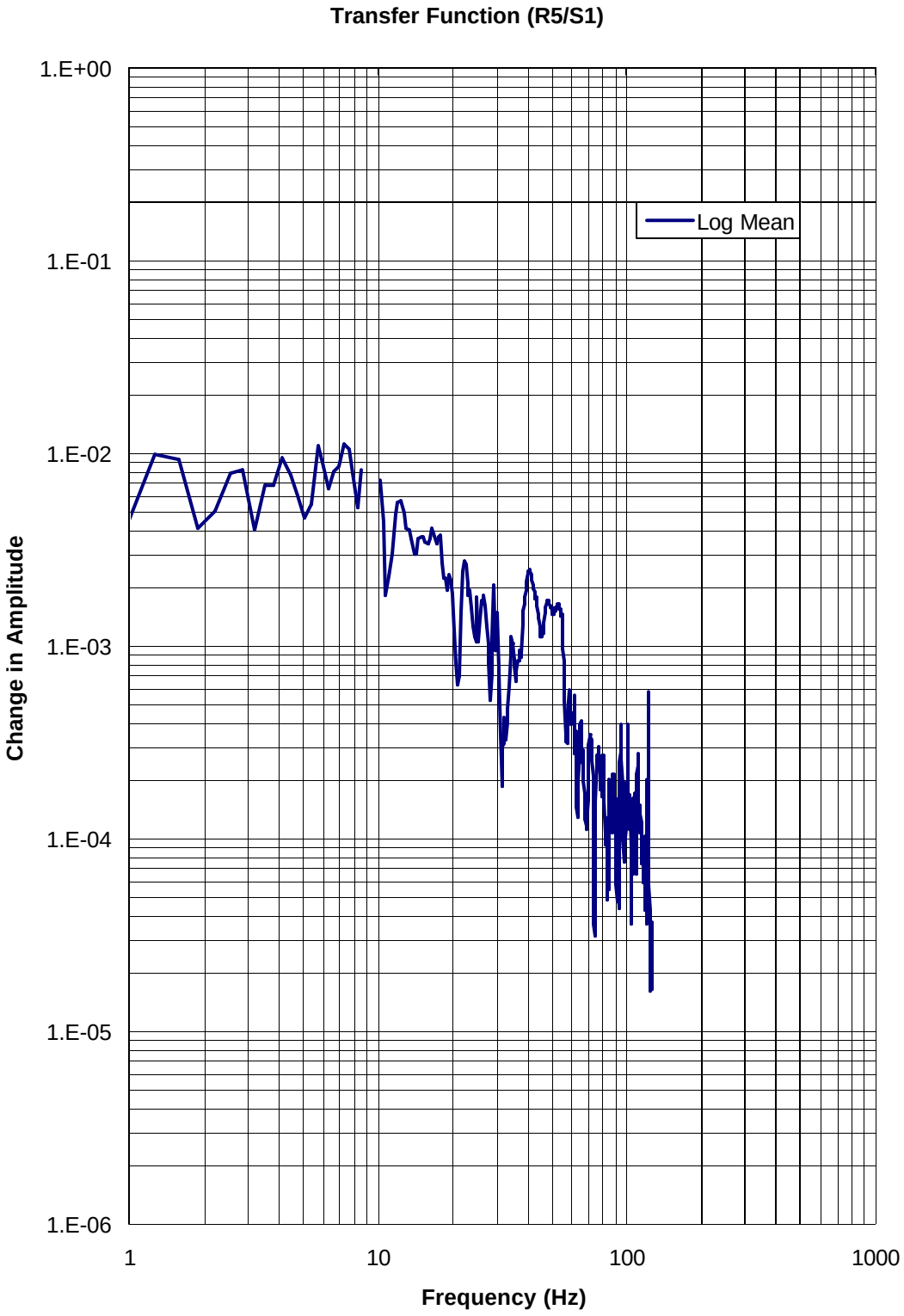

Figure 23: Ground Transmission - SLAC Cut-and-Cover Tunnel - 7 Aug 2002
Transmission from Drive Point S2 to Point in Tunnel R1

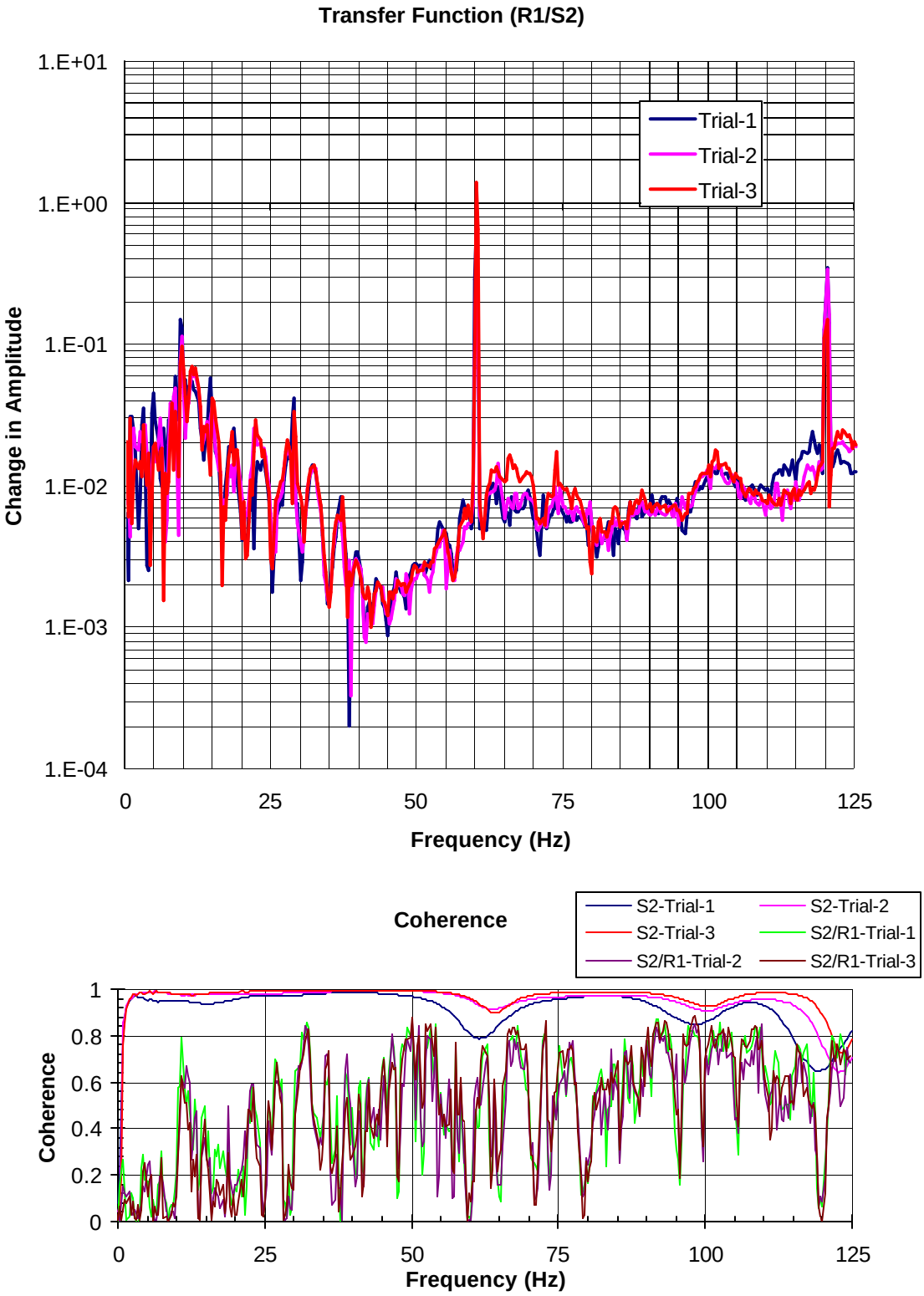

Figure 24: Ground Transmission - SLAC Cut-and-Cover Tunnel - 7 Aug 2002
Transmission from Drive Point S2 to Point in Tunnel R1

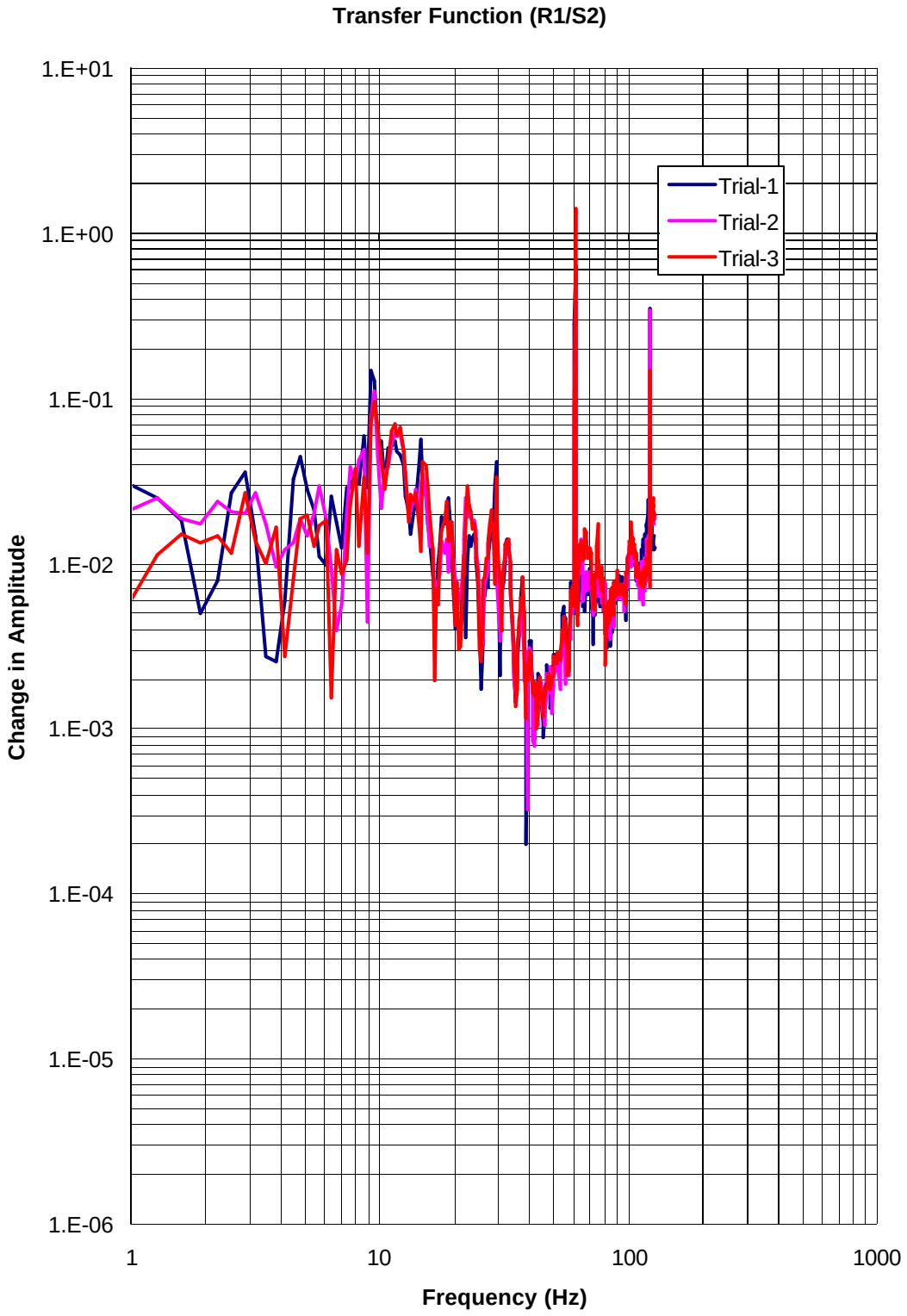

Figure 25: Ground Transmission - SLAC Cut-and-Cover Tunnel - 7 Aug 2002
Transmission from Drive Point S2 to Point in Tunnel R1

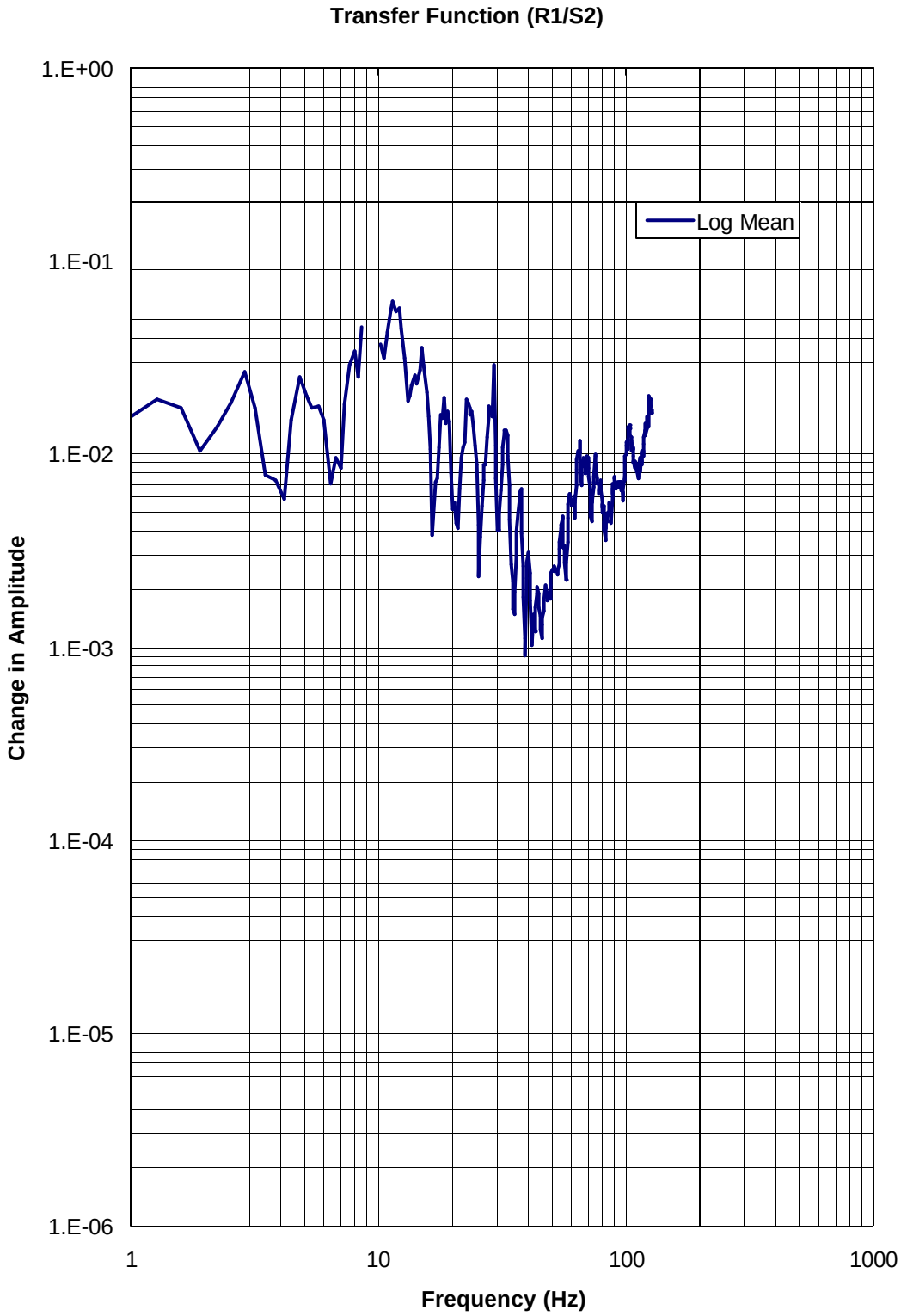

Figure 26: Ground Transmission - SLAC Cut-and-Cover Tunnel - 7 Aug 2002
Transmission from Drive Point S2 to Point in Tunnel R2

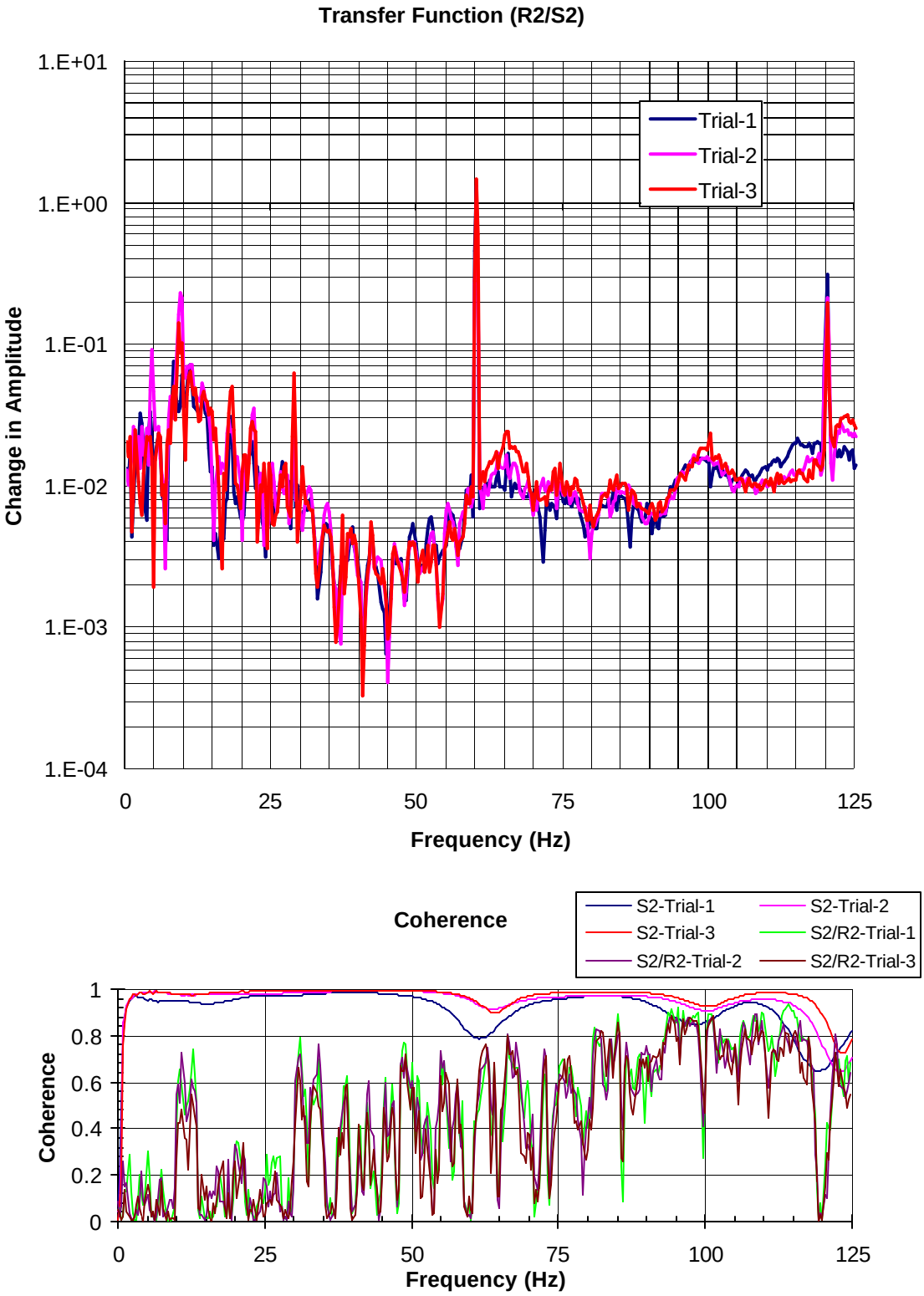

Figure 27: Ground Transmission - SLAC Cut-and-Cover Tunnel - 7 Aug 2002
Transmission from Drive Point S2 to Point in Tunnel R2

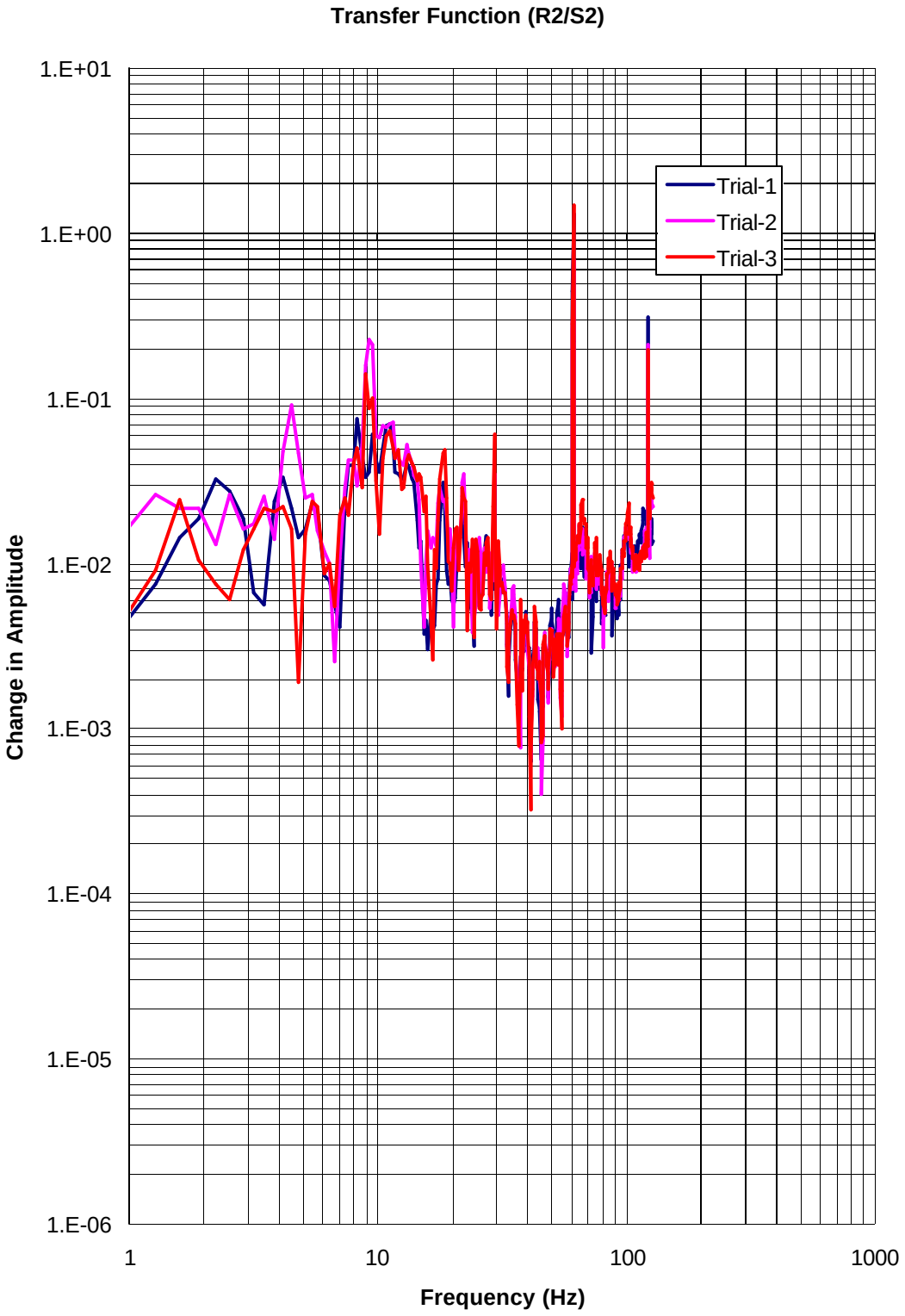

Figure 28: Ground Transmission - SLAC Cut-and-Cover Tunnel - 7 Aug 2002
Transmission from Drive Point S2 to Point in Tunnel R2

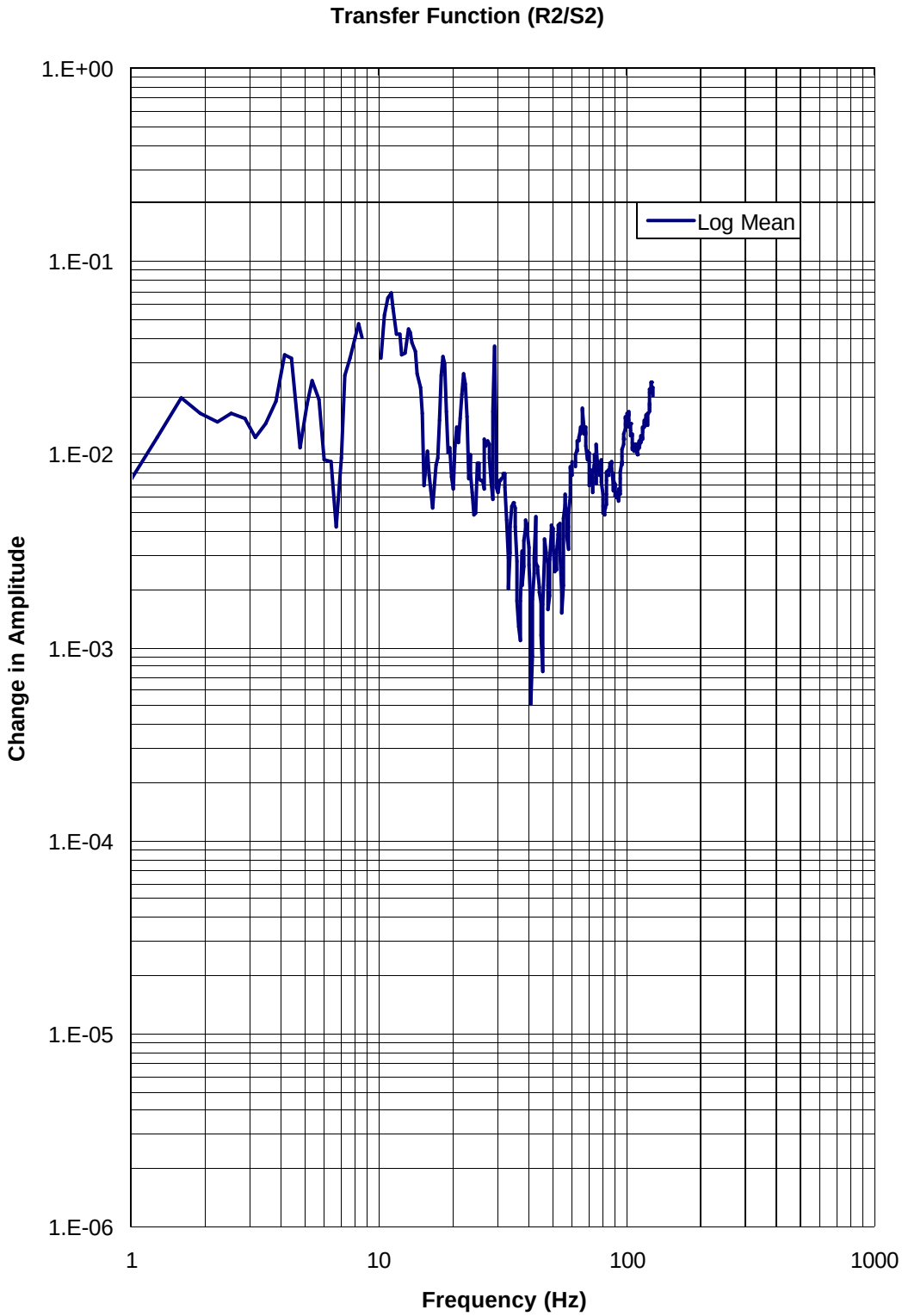

Figure 29: Ground Transmission - SLAC Cut-and-Cover Tunnel - 7 Aug 2002
Log Mean Transmission from Drive Point S1 - Summary

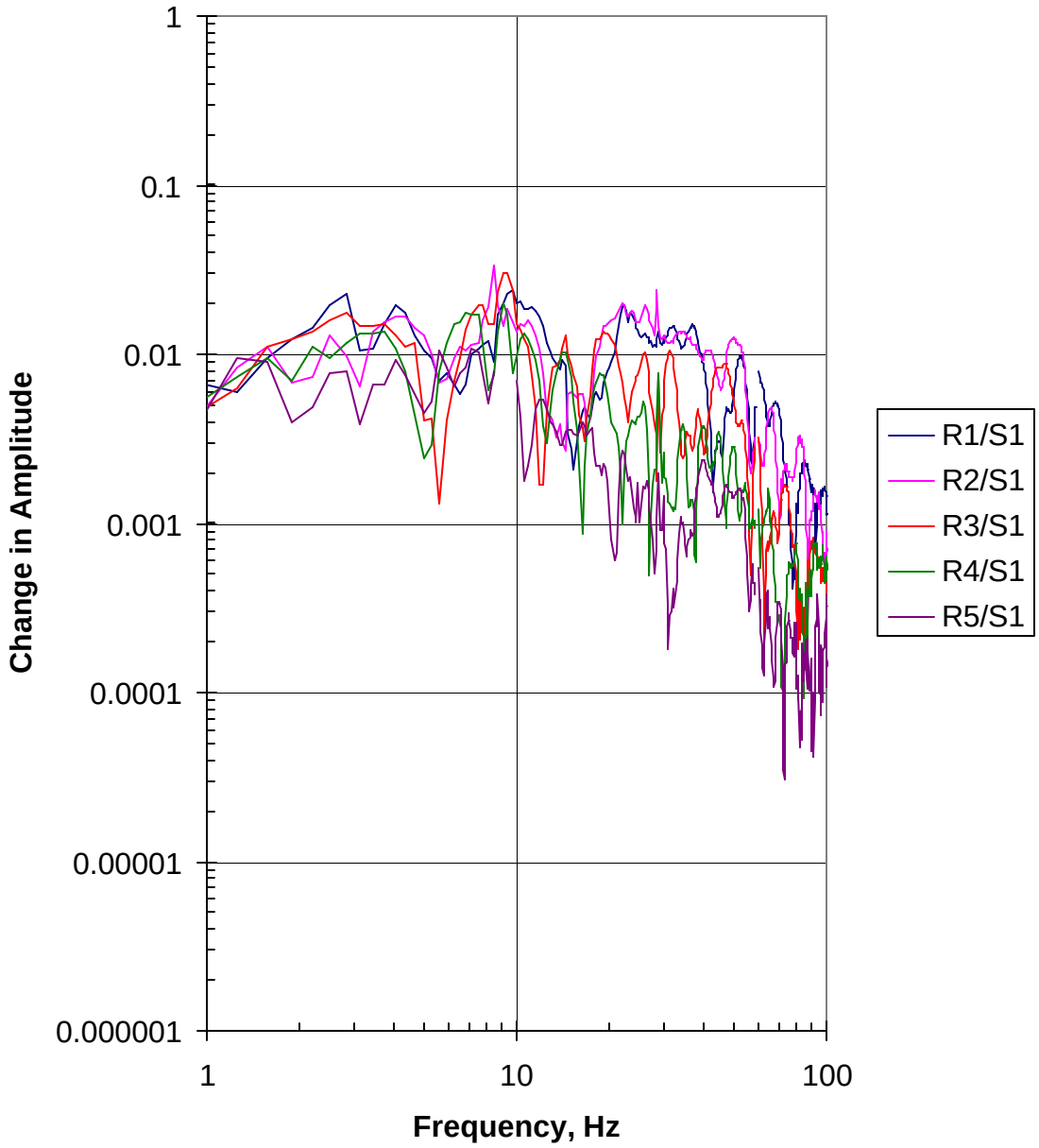

Figure 30: Ground Transmission - SLAC Cut-and-Cover Tunnel - 7 Aug 2002
Log Mean Transmission from Drive Point S1 - Summary
"Slightly Smoothed" (3.5 Hz)

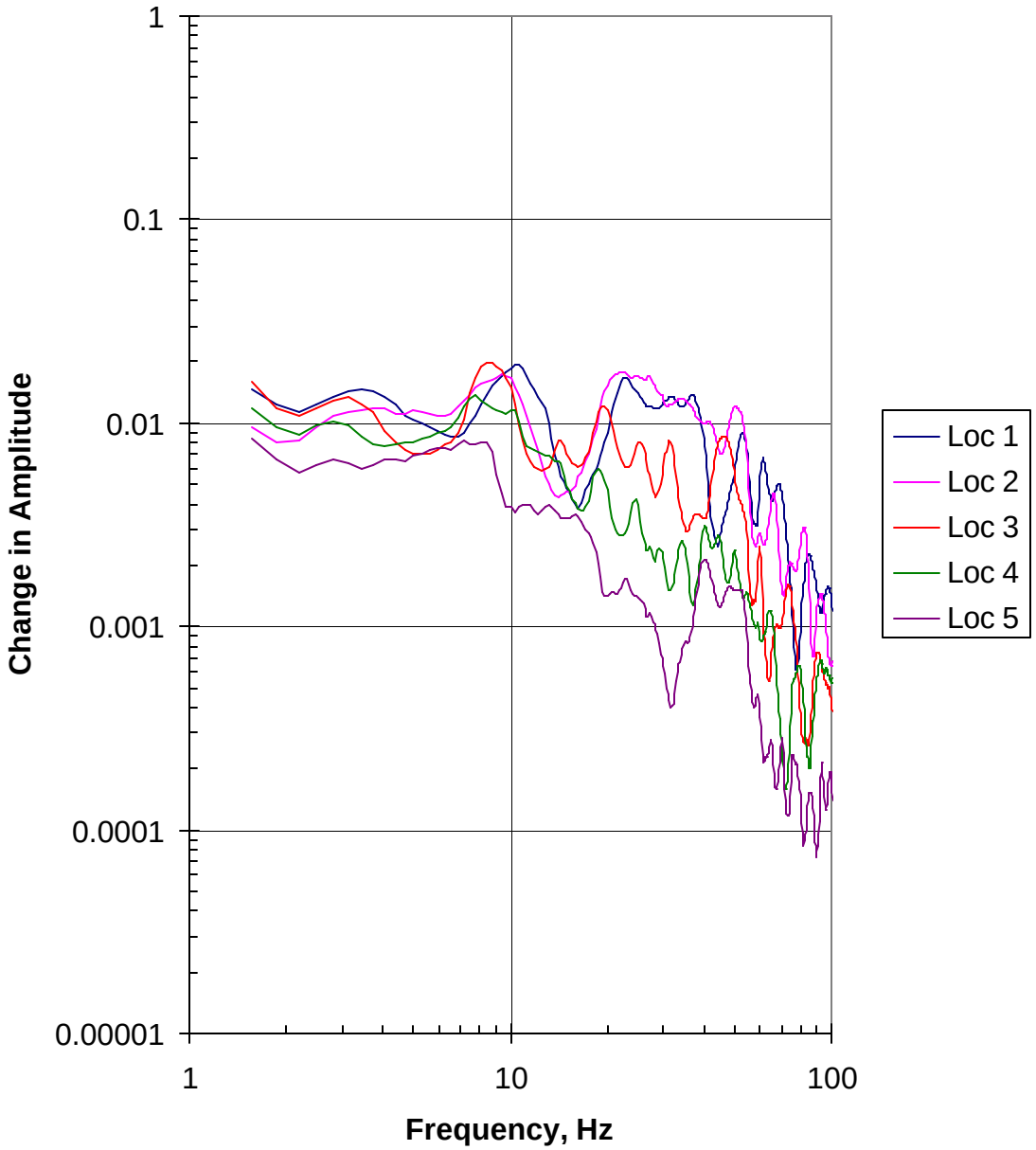

Figure 31: Ground Transmission - SLAC Cut-and-Cover Tunnel - 7 Aug 2002
Log Mean Transmission from Drive Point S1 - Summary
"Medium Smoothed" (6.5 Hz)

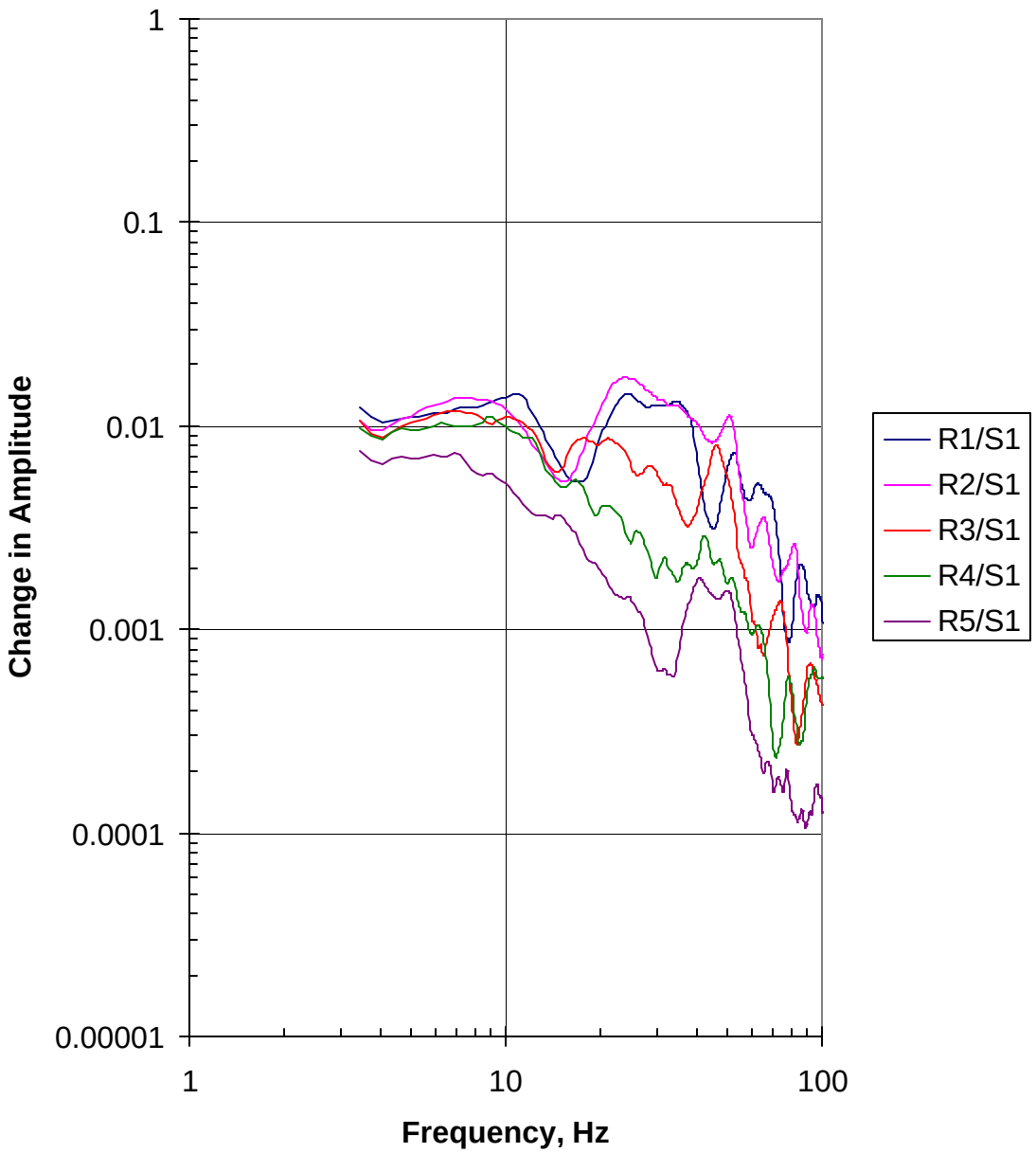

Figure 32: Ground Transmission - SLAC Cut-and-Cover Tunnel - 7 Aug 2002
Log Mean Transmission from Drive Point S1 - Summary
"Heavily Smoothed" (10 Hz)

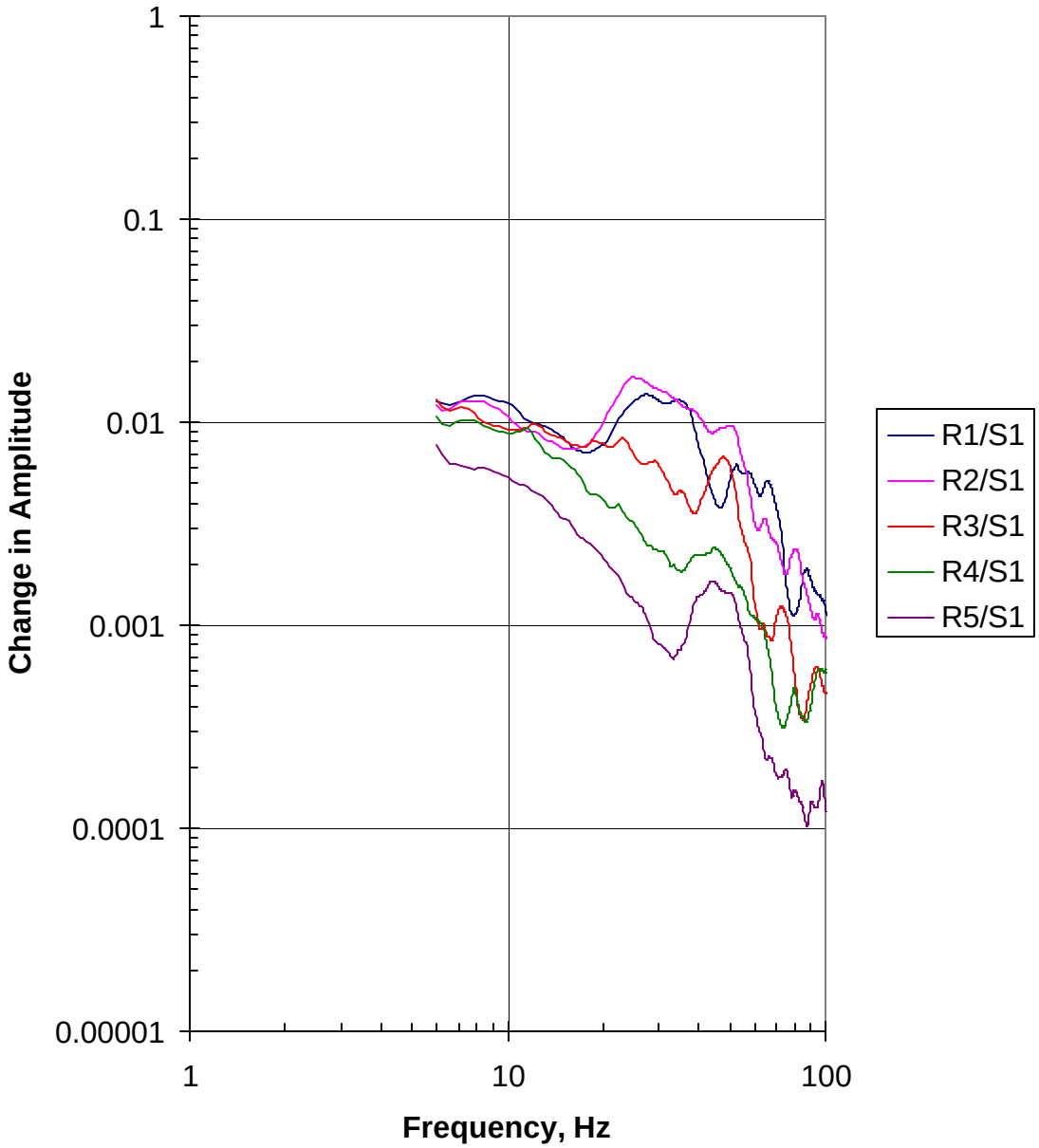

Figure 33: Ground Transmission - SLAC Cut-and-Cover Tunnel - 7 Aug 2002
Log Mean Transmission from Drive Point S2 - Summary

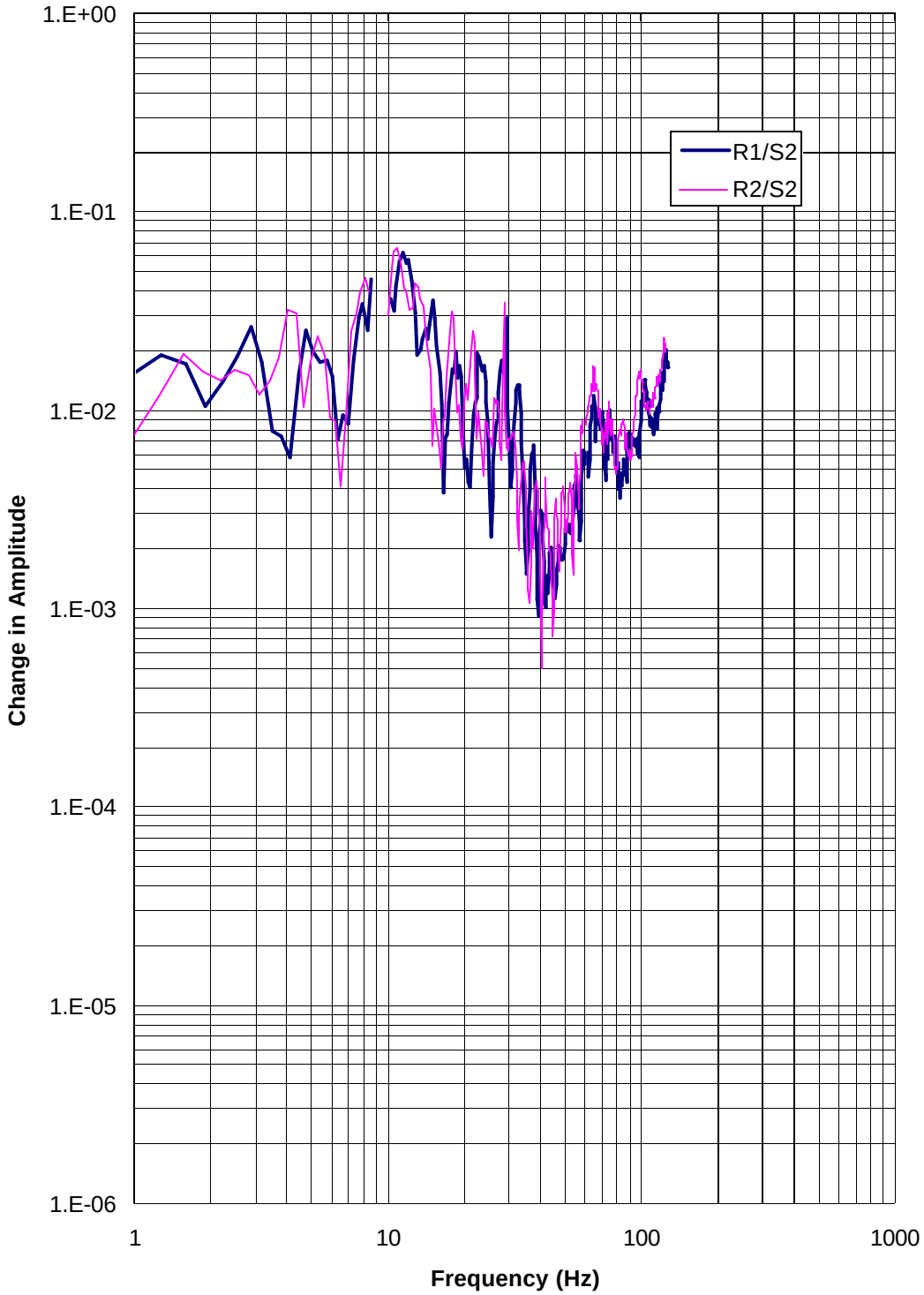

Figure 34: Ground Transmission - SLAC Cut-and-Cover Tunnel - 7 Aug 2002
Log Mean Transmission from Drive Point S2 - Summary
"Slightly Smoothed" (3.5 Hz)

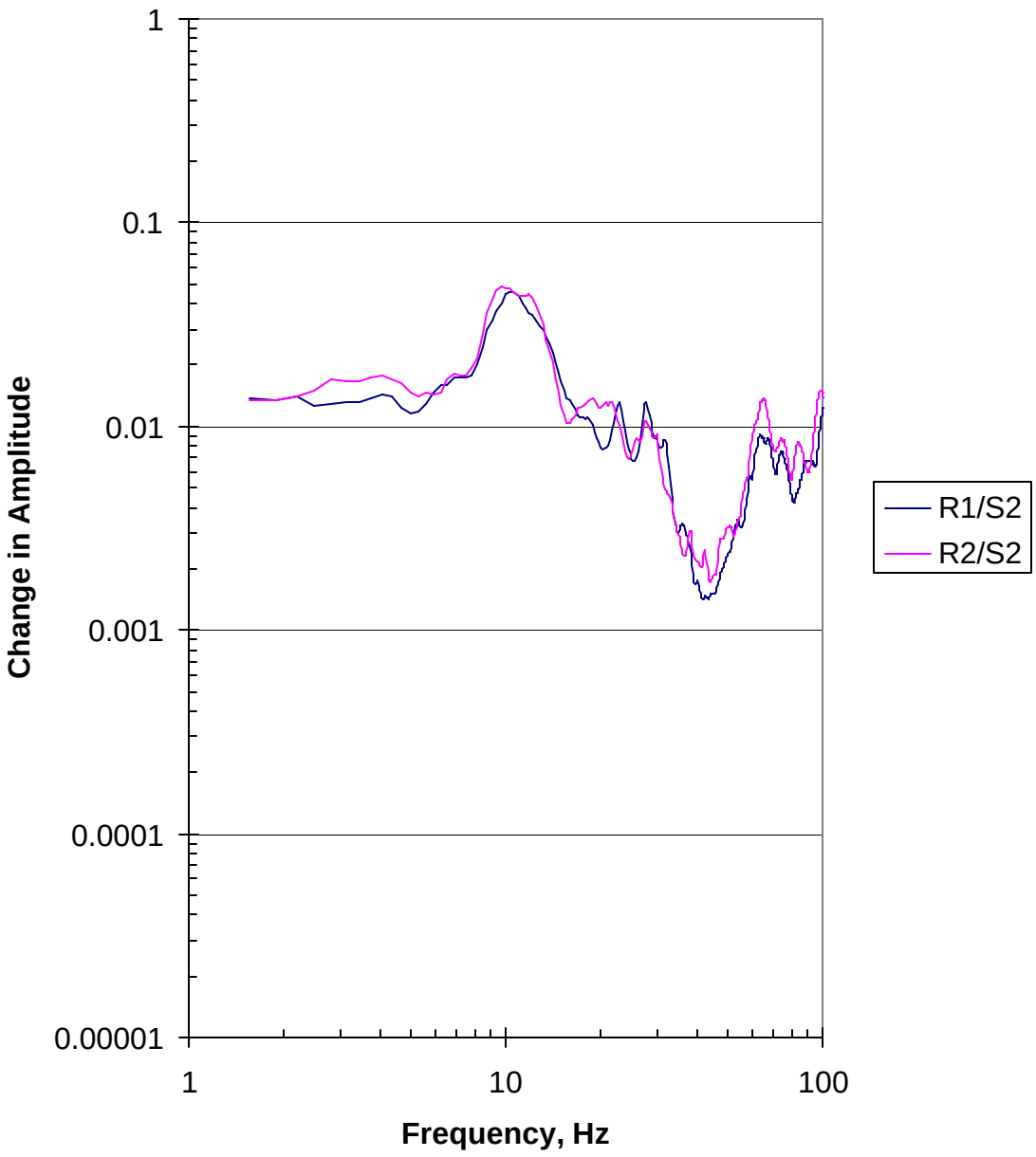

Figure 35: Ground Transmission - SLAC Cut-and-Cover Tunnel - 7 Aug 2002
Log Mean Transmission from Drive Point S2 - Summary
"Medium Smoothed" (6.5 Hz)

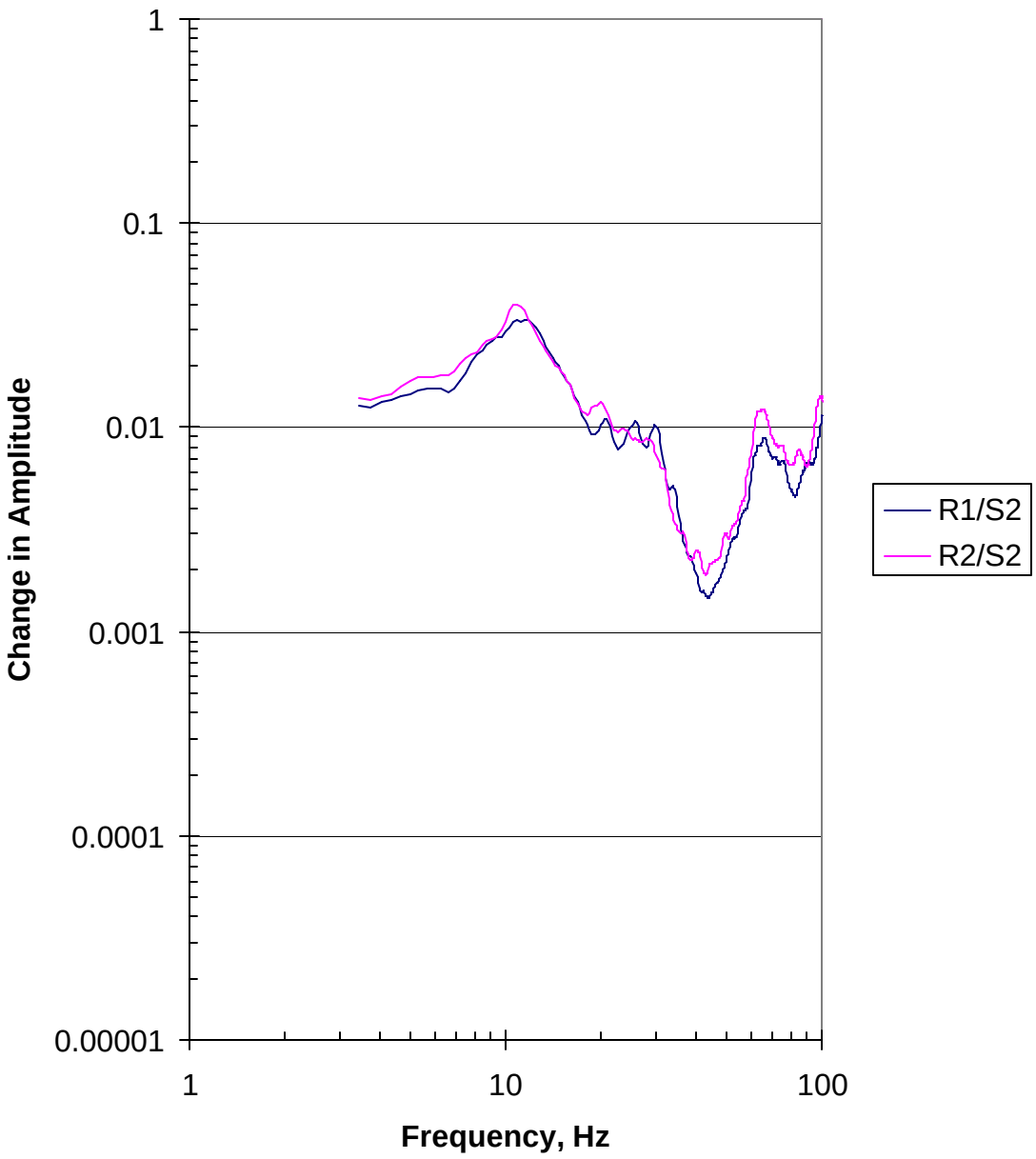

Figure 36: Ground Transmission - SLAC Cut-and-Cover Tunnel - 7 Aug 2002
Log Mean Transmission from Drive Point S2 - Summary
"Heavily Smoothed" (10 Hz)